DANMARKS OG GRØNLANDS GEOLOGISKE UNDERSØGELSE RAPPORT 2019/39

Greenlandic Ice Cap Water

Technical Report on five potential locations for meltwater export for the 2nd licensing round

Andreas P. Ahlstrøm, Christian N. Albers, Kristian K. Kjeldsen,
Anders R. Johnsen, Signe H. Larsen, Peter Lisager, Martin Nauta,
Kenneth D. Mankoff, Tina Bundgaard Bech, Bent Hasholt,
Danielle Hallé, Karina Hansen, Signe B. Andersen,
Camilla S. Andresen, Michele Citterio,
Robert S. Fausto & Anne M. Solgaard

GEOLOGICAL SURVEY OF DENMARK AND GREENLAND
DANISH MINISTRY OF CLIMATE, ENERGY AND UTILITIES

DANMARKS OG GRØNLANDS GEOLOGISKE UNDERSØGELSE RAPPORT 2019/39

Greenlandic Ice Cap Water

Technical Report on five potential locations for meltwater export for the 2nd licensing round

Andreas P. Ahlstrøm, Christian N. Albers, Kristian K. Kjeldsen,
Anders R. Johnsen, Signe H. Larsen, Peter Lisager, Martin Nauta,
Kenneth D. Mankoff, Tina Bundgaard Bech, Bent Hasholt,
Danielle Hallé, Karina Hansen, Signe B. Andersen,
Camilla S. Andresen, Michele Citterio,
Robert S. Fausto & Anne M. Solgaard

GEOLOGICAL SURVEY OF DENMARK AND GREENLAND
DANISH MINISTRY OF CLIMATE, ENERGY AND UTILITIES

GEUS

Contents

1. Summary

This report contains information on five selected locations that may be utilized for industrial collection of drinking water, and provides the technical background for the second licensing round of the Greenland Government in its Strategy for Export of Ice and Water. This report is not aimed at addressing any technical or engineering questions posed by the locations or water treatment, but only concerns the natural environment and the quality of the water as it was sampled. A prerequisite in the investigation has been that the water should be at least partly derived from meltwater originating either from the Greenland Ice Sheet or from local glaciers and ice caps. The identification and selection process for locations was described in detail in Ahlstrøm et al. (2018) and updated in Kjeldsen et al. (2019). Locations are defined as outlets of a significant meltwater river to accessible fjords in the southwestern part of Greenland, to minimize potential sea ice and iceberg interference. Catchments for each location or river outlet were derived employing advanced hydrological methods, using the most recent elevation models available.

The five selected locations represent different catchment sizes with varying amounts of discharge, ranging from roughly 290,000 million litres per year, down to slightly over 10,000 million litres per year. The rivers at all locations are, on average, discharging water from May to November with the vast majority of water discharging in the period June-September. A comparison between modelled discharge for the catchments for the two periods 1980-1991 and 2006-2017, showed an increase in the discharge at all sites except one, which was stable. A similar method was also used to examine the change in discharge over the last few decades, showing a promising overall melt increase of more than 50 % for the region.

The five selected locations were visited by boat to sample the water and collect additional data. The field visits were conducted in June and September in either 2018 or 2019, to capture the seasonal variability in the water quality. Two locations drain ice sheet catchments and three locations drain catchments with local mountain glaciers and ice caps.

An extensive analysis of chemical, physical and microbiological parameters was performed on the water samples. Some types of analyses had to be performed on-site, some were performed at GEUS laboratories, and some at certified commercial laboratories.

All of the locations provide large amounts of meltwater during the summer from June-September, with river outlets being relatively near deep fjord waters. The meltwater contains varying amounts of sediment derived from glacier erosion of the bedrock, requiring filtration of the meltwater before use. For all five locations, inorganic parameters are below drinking water requirements and guidelines in filtered water samples. Gentle UV-treatment of the water is recommended, as is commonly required for surface water, as microbiological parameters generally exceed the guideline limits at all locations.

While the water quality can be expected to vary over the season, the results provide a strong indication of the potential for export of drinking water from meltwater rivers in Greenland.

2. Introduction

Drinking water of high quality is becoming a scarce resource worldwide. As the world population grows, demand is rising while the supply is under pressure from the impact of climate change. In Greenland, pure meltwater running off the Greenland Ice Sheet and local glacier and ice caps provides the solution. As the annual hydrological cycle intensifies with higher temperatures in the Arctic, the available water resource only increases. Unlike mountain glaciers which are vanishing globally, the Greenland Ice Sheet is vast, containing 2.85 million cubic kilometres of pure glacier ice providing a freshwater reservoir without equal in the northern hemisphere.

The Greenland Ice Sheet covers most of the land in Greenland with rivers transporting the meltwater a short distance through the mountains to the fjords through the largely uninhabited country. Due to limited sea ice, the fjords in Southwest Greenland provide direct access by ship to the meltwater river mouths.

The Government of Greenland actively supports the prospect of drinking water export from this immense resource. To attract investments from the industry, an extensive effort has been launched to map possible extraction locations, determine the quality of the meltwater and review the existing ice and water export legislation.

Mapping and water quality assessments are undertaken by the Geological Survey of Denmark and Greenland (GEUS) adhering to the highest international standards. GEUS has been contracted by the Government of Greenland to identify suitable locations for extraction of drinking water from meltwater rivers, conduct field investigations and water sampling, and subsequently, carry out water quality assessments in certified laboratories. GEUS is the National Data Centre for water quality information for all of Denmark's more than 280,000 drinking water wells and has carried out extensive geoscientific fieldwork in Greenland since 1946.

3. Selection of potential locations

Locations are defined as outlets of significant meltwater rivers to accessible fjords in the southwestern part of Greenland, to minimize potential sea ice and iceberg interference. The initial assessment of locations was based on a three-level approach, evaluating in turn *accessibility*, *abundance*, and *water quality*, respectively. For each of these three levels, different criteria were identified and assigned a weight in the assessment with the goal to single out the most promising locations to visit in the field.

The *accessibility* criteria include proximity to infrastructure, marine chart coverage, availability of bathymetry data, abundance of sea ice and icebergs, and river slope, respectively. The *abundance* criteria relate to water discharge, length of the melt season, existence of proglacial lakes, risk of outburst floods, upstream catchment changes, total ice cover within the catchment, and the ice cover relative to the size of the catchment, respectively. Finally, the *water quality* criteria focus on origin of the water, age of the source ice, expected sediment concentration in the meltwater, and other issues from contact with naturally occurring minerals.

The selection of potential location is a two-phase process. In the first part each location was meticulously examined and rated with respect to the 18 criteria from the considerable geospatial, geological and geochemical datasets available to the Government of Greenland and GEUS. The criteria, sorted by level, and their graduation and weight are illustrated in Table 1. The rating of a location assigns a number, moderated by a relative weight, for each criterion. In the second phase potential locations and their catchments have been assessed manually. This was to prevent inclusion of catchments that may appear promising in relation to the criteria, but where one or more factors would lead to the conclusion that it would be unviable to include the specific site in the final selection group. The final outcome of the two phases is the ranking of the locations, which in turn is used to select the most promising locations to visit in the field for water sampling and further data collection.

Figure 1 illustrates an overview of the final selected locations.

Criterion		Poor 5	Mainly poor 4	Useful 3	Mainly good 2	Good 1	Weight
Accessibility	Proximity to infrastructure	Unknown/sporadic access from marine/land side and/or >100 km	Occasional access from the marine side in the operational part of the season, and/or >100 km	Access possible from marine side in the operational part of the season	<25 km with access possible from the marine side all year round	Access by road all year round	Low
	Marine chart coverage	No charts	In proximity of older charts	In proximity of recent charts	Older charts	Recent charts	Low
	Bathymetry	Known shallow waters	No nearby data - estimated risk of shallow waters	No nearby data - estimated deep waters to the coast	Assumed deep water to coast based on experience and nearby data	Deep waters directly to the coast known	High
	Sea ice	Occasional blocking sea ice and fjord ice	Occasional blocking fjord ice	Occasional blocking sea ice	Narrow fjord access, ice-free ocean	Open fjord, ice-free ocean	High
	Icebergs	In fjord with calving glacier and some icebergs in ocean	In fjord with minor calving glacier and some icebergs in ocean	In fjord with minor calving glacier and few icebergs in ocean	No calving glacier in fjord and some icebergs in ocean	No calving glacier in fjord and few icebergs in ocean	High
	River slope over the lowermost 500 m	0 – 0.005 m/m	0.005 – 0.025 m/m	0.025 – 0.050 m/m	0.050 – 0.100 m/m	> 0.100 m/m	High
Abundance	Discharge	Small catchment with no ice cover	Small catchment with partial ice cover	Large catchment with minor ice cover	Large catchment with partial ice cover	Very large catchment with partial inland ice sheet cover	Medium
	Length of melt season	Northwestern	Western	Southwestern	Southern, with small lake	Southern, with large lake	Medium
	Proglacial lake	No lake	Small lake	Several small lakes	Large lake	Several large lakes	Medium
	Outburst floods	Clear indications of outburst flood from lake	Likely outburst flood from lake	Lake with adjoining ice cover, but outburst flood less likely	Outburst flood not likely, but small lake with adjoining ice cover	No lakes with adjoining ice cover	High
	Catchment change	Small catchment with significant risk of change	Small catchment with some risk of change	Large catchment with risk of change	Large catchment with low risk of change over ice cover	Very large catchment on the inland ice (change not important)	Medium
	Total ice cover in catchment	0 – 4 km^2	4 – 8 km^2	8 – 15 km^2	15 – 30 km^2	> 30 km^2	High
	Ice cover relative to catchment size	0 – 10 %	10 – 15 %	15 – 20 %	20 – 30 %	> 30 %	High
Water quality	Origin of water	Primarily from ice-free catchment	Primarily from local ice cover (not inland ice)	Both from local glaciers and inland ice	Primarily meltwater from the inland ice	Almost exclusively meltwater from the inland ice	Low
	Age of ice source	Minor local glacier	Primarily from local ice cap	Both from local glaciers and inland ice	Younger inland ice	Older inland ice	Low
	Sediment concentration	Extremely high (>2000 mg/L)	High (1000-2000 mg/L)	Medium (300-1000 mg/L)	Low (50-300 mg/L)	Weak (<50 mg/L)	Low
	Radioactivity	High concentration	Medium-high concentration	Medium concentration	Medium-low concentration	Low concentration	High
	Inorganic compounds	High concentration	Medium-high concentration	Medium concentration	Medium-low concentration	Low concentration	High

Table 1. *The 18 criteria sorted by the three levels (accessibility, abundance and water quality) and the specific graduation into five levels. The column to the right assigns a weight to each criterion with respect to the others.*

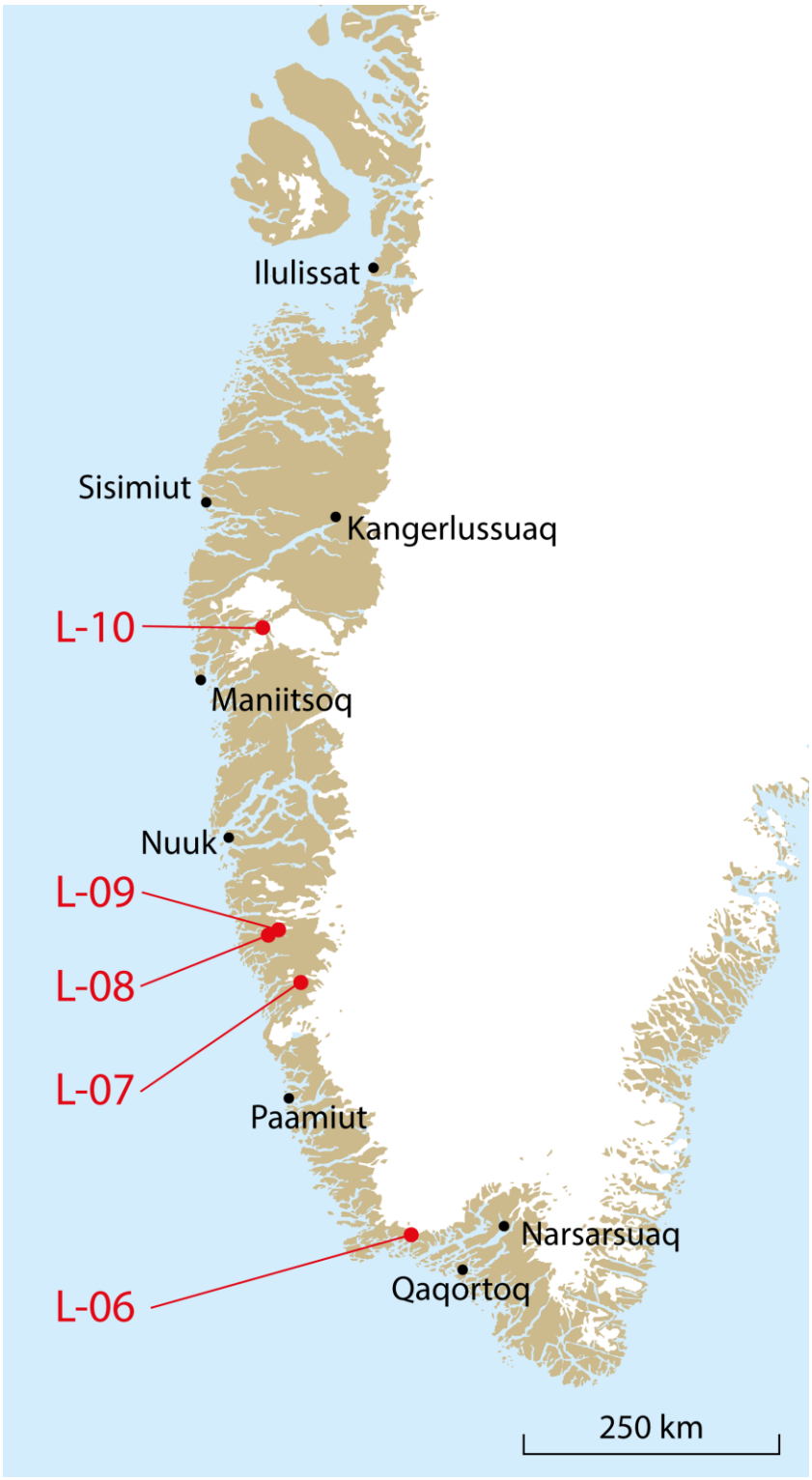

Figure 1. *Overview map showing the five selected locations (red dots) as well as larger cities and airports in the region of interest.*

4. Accessibility assessment

An intimate knowledge of the sailing conditions is crucial in order to determine whether a location is suitable for meltwater collection. Primary parameters to be assessed includes bathymetry, nearby ports, fjord ice conditions, sea ice and iceberg occurrence, which together determine what kind of ship or vessel is appropriate for a given location. Currently, five ports in South and Southwest Greenland, i.e. in the vicinity of the selected locations, service shipping over the Atlantic Ocean: Sisimiut, Nuuk, Narsaq, Qaqortoq and Nanortalik. These ports have a maximum capacity between 550 and 3300 TEU. The most proximate port to most locations is Nuuk, which is also the largest of the ports.

4.1 Sea ice and iceberg conditions

Conditions for sea ice and icebergs vary over the extensive south-western Greenland coastline. In South Greenland, the ice present mainly consists of sea ice and glacier ice transported down along the East Greenland coast with the East Greenland current where it eventually flows around Kap Farvel (Cape Farewell). South Greenland is generally free from sea ice from August to December, while icebergs can be expected year-round. Unlike the sea ice in South Greenland, the sea ice in Southwest Greenland is produced locally during the winter. Icebergs are present year-round, but more so to the north near Disko Bay, where calving glaciers are more proliferate. According to the Danish Meteorological Institute (DMI), it is normally possible to sail to Aasiaat and Ilulissat from around May to December. The monthly mean concentration of sea ice around Greenland for the time period 2000-2010 is shown in Figure 2, which illustrates the difference between South and Southwest Greenland and also that a significant part of the coast towards Disko Bay remains relatively ice free for significant parts of the year. Still, icebergs are present year-round. All the locations selected are situated in the part of Greenland least affected by sea ice and icebergs, and thus optimal for transportation and the length of extraction season, evaluated on the basis of the maps shown in Figure 2 and maps from DMI's ice mapping service in the Kap Farvel region and south-western Greenland for the period April 2010 to February 2017.

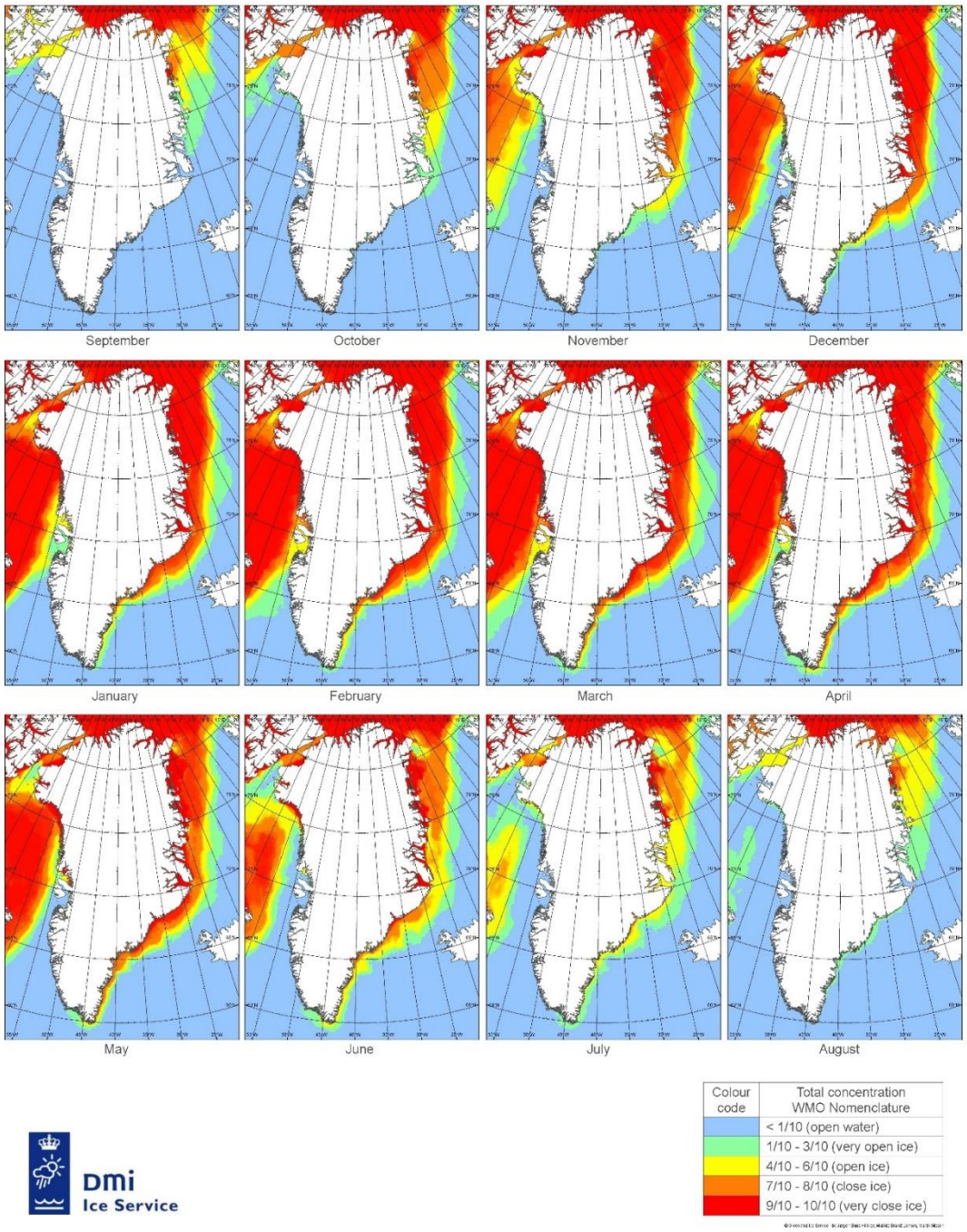

Figure 2. *Monthly mean sea ice concentration derived from Greenland overview ice charts over the period 2000-2010.*

4.2 Bathymetry

The international bathymetric surveying carried out around Greenland (IBCAO, International Bathymetric Chart of the Arctic Ocean) does not cover the Greenlandic fjords adequately. Generally, routing of larger vessels take place only through regions with bathymetric charts suitable for navigation. By special agreement with the Danish Geodata Agency we have been granted access to yet unpublished bathymetric charts for the regions where

these are so far available. A more thorough survey of the fjords in Greenland is currently underway, but not yet completed. To ensure the best possible evaluation of the access to the selected locations, we also included unpublished water depth observations collected from a range of sources by the Greenland Institute of Natural Resources (K. Brix Zinglersen). These water depth data cover a wider region than the bathymetric charts of the Danish Geodata Agency and are often the only data source in the vicinity of the selected locations. However, these data are not tied to a vertical reference surface (e.g. MSL, LAT, geoid, ellipsoid), implying that no corrections, e.g. tidal corrections, etc., have been applied, but generally just indicates the water depth below a ship at a given time. Thus, data should be used with caution and only as an indication of accessibility of a given location and not for navigational purposes.

Summarizing, the observations of water depth presented below are derived from three datasets:

1. A dataset from the Greenland Institute of Natural Resources, which consists of single beam water depth data from tour boats and trawlers recorded during navigation, not originally intended as bathymetric measurements. These are generally depicted as lines, or rather a series of point measurements. Kindly provided by Karl Brix Zinglersen (GNRI).
2. A bathymetric dataset from the Danish Geodata Agency recorded with multibeam sonar. These data provide full areal coverage when available. Kindly provided by Danish Geodata Agency.
3. A dataset resembling (1) above, recorded from the boat during fieldwork.

Note that datasets (1) and (3) are not proper bathymetric datasets and have not been corrected for tidal water level differences. They are only intended to provide an indication of the likely accessibility by ship and may not be relied on for actual navigational purposes. The water depth presented in Figure 4 through Figure 13 illustrate the minimum water depth within 100 m x 100 m grid cells, except close to the river outlet where the individual sampled depth is shown as points. Contours mark the 2 m vertical equidistance.

Moreover, to supplement the assessment of the bathymetry we incorporate available nautical maps, though recognizing that their accuracy may be questionable. Thus, most emphasis is on the bathymetrical datasets during the selection phase. The map coverage is illustrated in Figure 3.

In addition to the above listed datasets, ASIAQ joined the June 2019 field campaign to collect bathymetrical data near locations L-07, L-08, L-09 and L-10. The data was collected using a single-beam echosounder attached with a RTK radio-link to a close by GNSS station. The static GNSS station was setup by ASIAQ during the field campaign and provided correction data for the position of the echosounder; both in the horizontal plane, but also tidal correction for the vertical depth measurements. For consistency, the data points are color-coded to match the fjord bathymetry data, but 2 m contour lines at each site is also provided. Note that the data from ASIAQ is referenced to the GVR2016 vertical frame and depth measurements have an anticipated accuracy of < 20cm.

We note that at some locations there is limited information on the bathymetry, however, satellite imagery of the fjord/river interface is provided to illustrate the conditions.

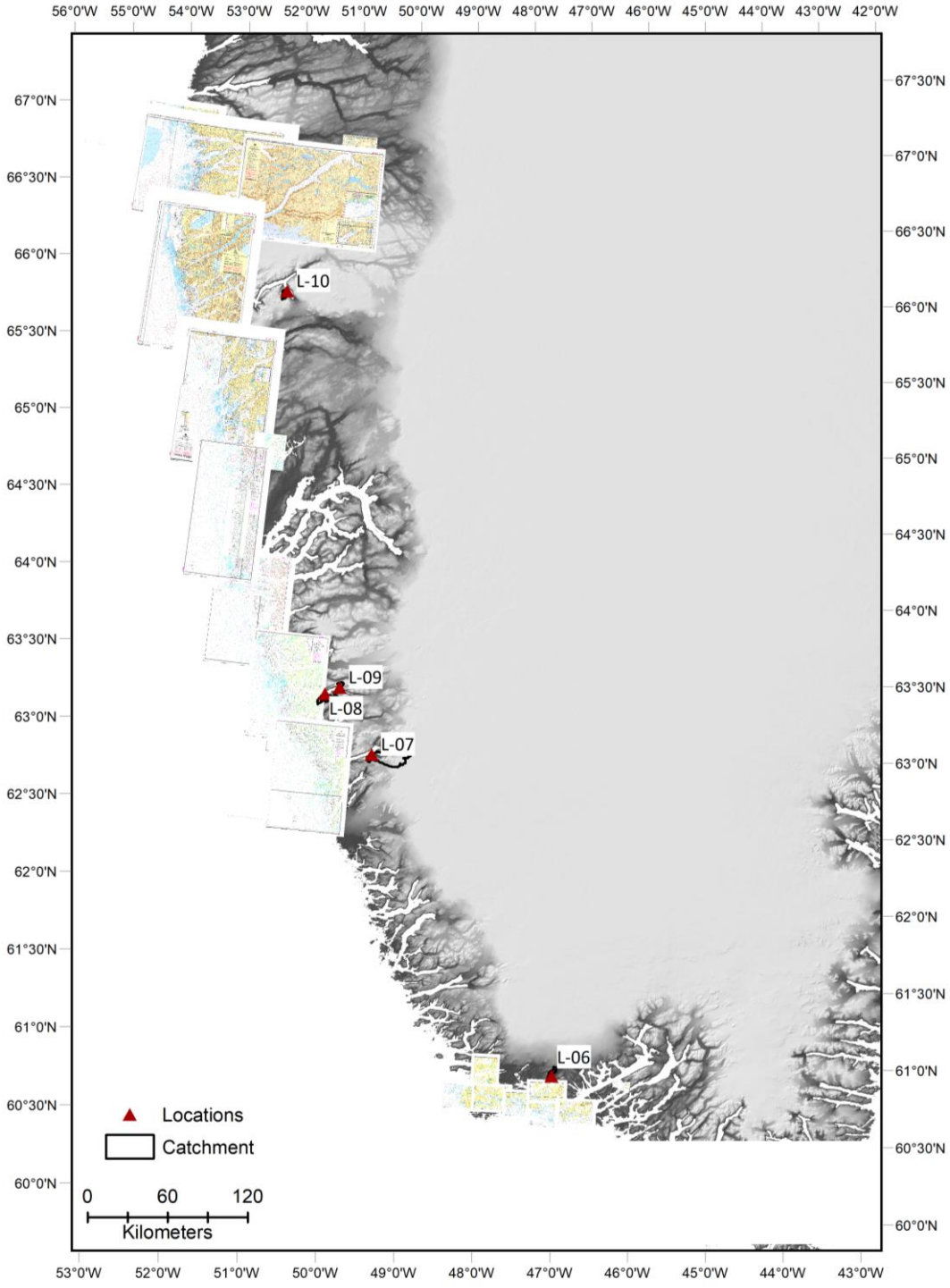

Figure 3. *Overview map showing the availability of nautical maps used during the selection process.*

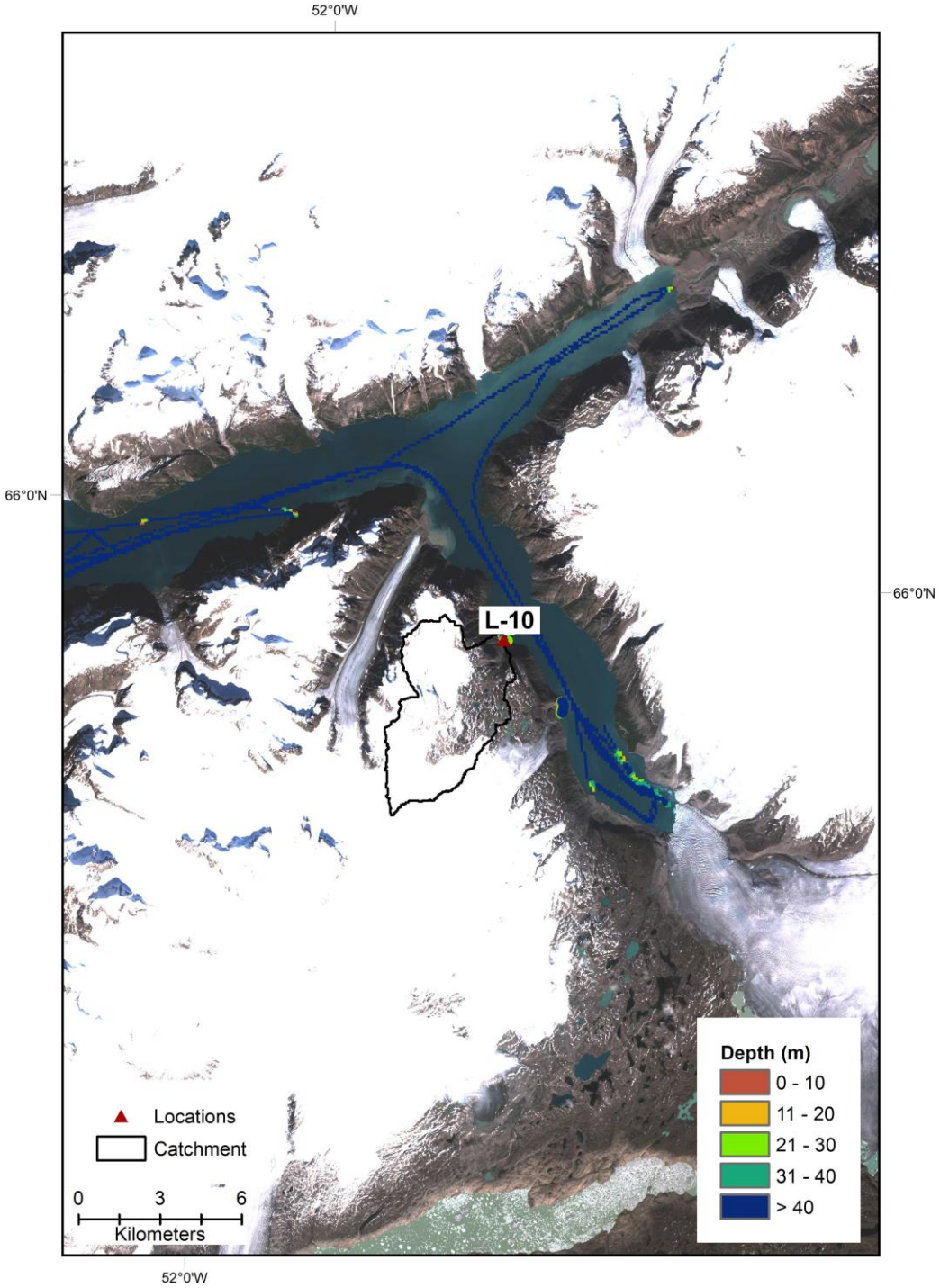

Figure 4. *Location L-10. Map showing the location of the river outlet (red triangles) and accompanying catchments (as a black line). The colour scale indicates approx. water depth from four different sources of data described in detail the text. Depth relates to the minimum water depth within 100 m x 100 m grid cells, except close to the river outlet where the individual sampled depth is shown as points.*

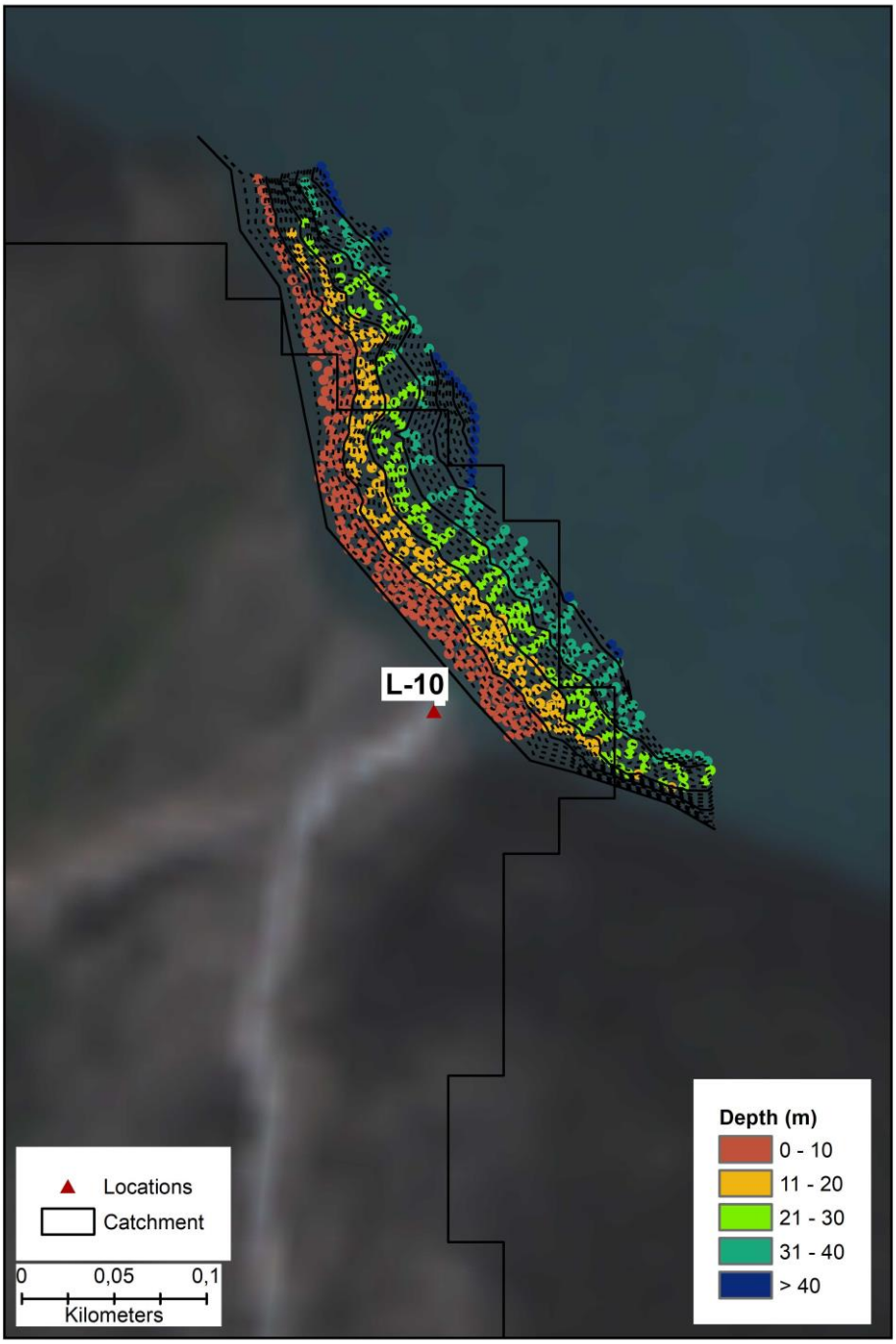

Figure 5. *Close up of Location L-10. Map showing the location of the river outlet (red triangles) and accompanying catchments (as a black line). The colour scale indicates approx. water depth from four different sources of data described in detail the text. Depth relates to the minimum water depth within 100 m x 100 m grid cells, except close to the river outlet where the individual sampled depth is shown as points. Contours mark the 2 m vertical equidistance.*

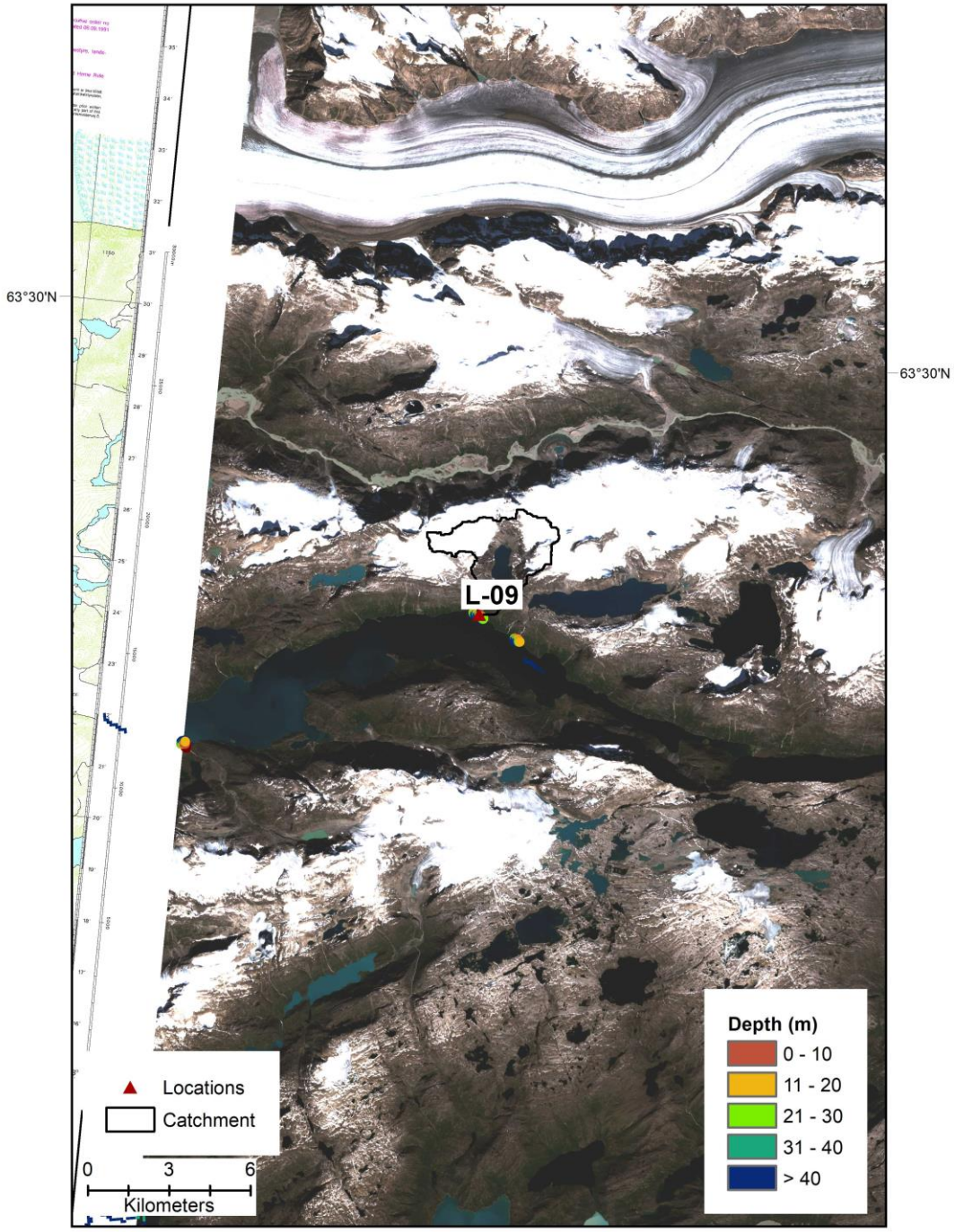

Figure 6. *Location L-09. Map showing the location of the river outlet (red triangles) and accompanying catchments (as a black line). The colour scale indicates approx. water depth from four different sources of data described in detail the text. Depth relates to the minimum water depth within 100 m x 100 m grid cells, except close to the river outlet where the individual sampled depth is shown as points. Contours mark the 2 m vertical equidistance.*

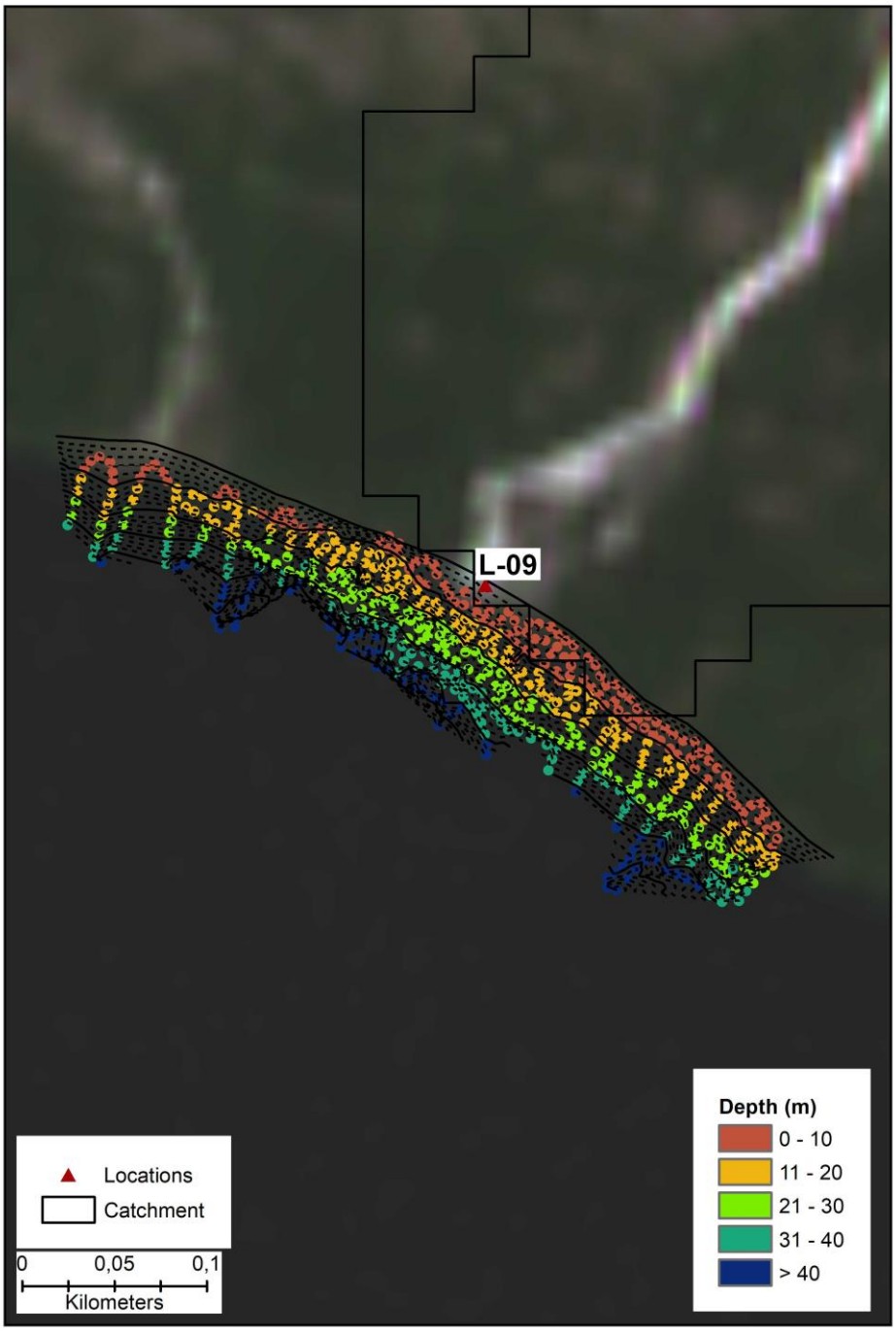

Figure 7. *Close up of location L-09. Map showing the location of the river outlet (red triangles) and accompanying catchments (as a black line). The colour scale indicates approx. water depth from four different sources of data described in detail the text. Depth relates to the minimum water depth within 100 m x 100 m grid cells, except close to the river outlet where the individual sampled depth is shown as points. Contours mark the 2 m vertical equidistance.*

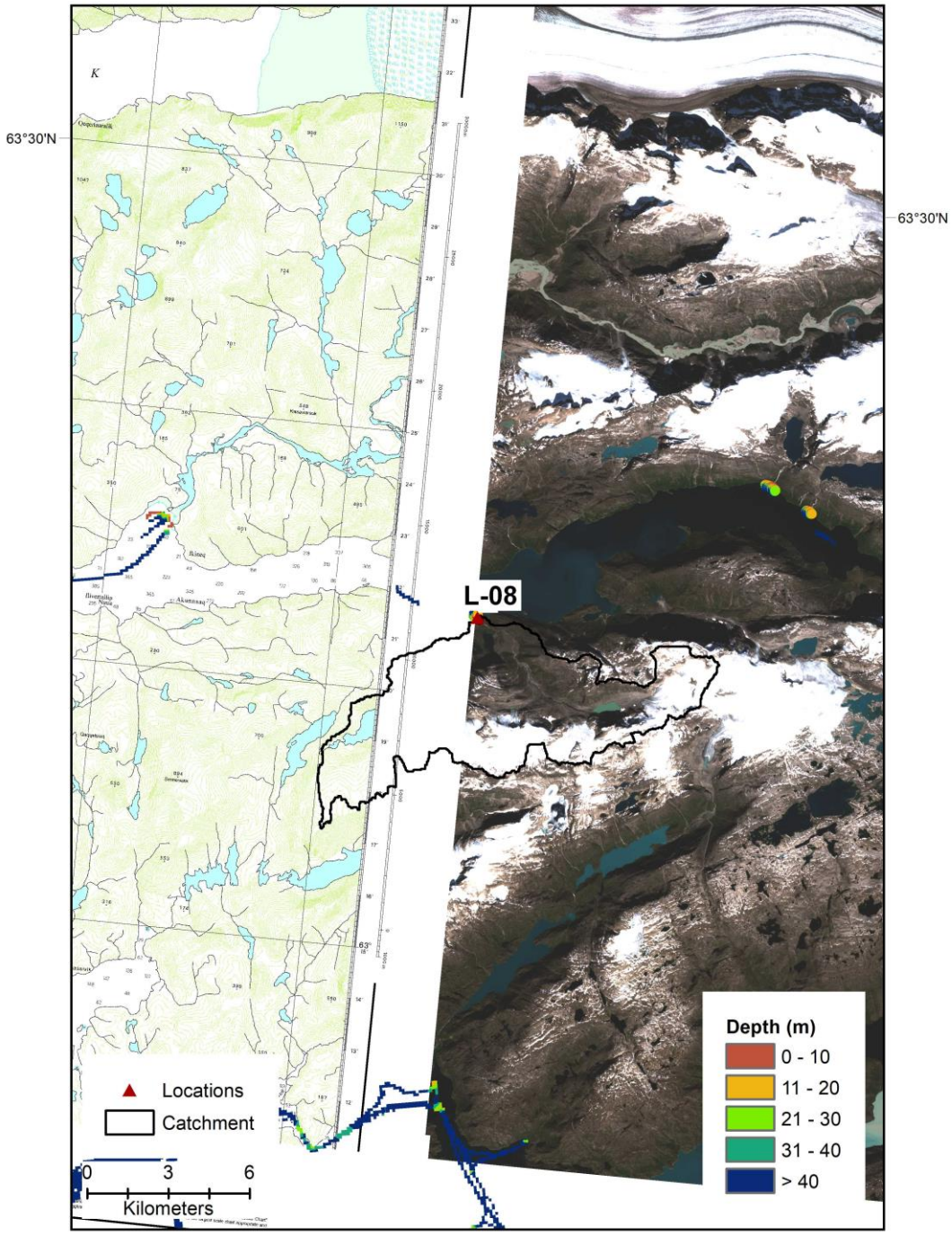

Figure 8. *Location L-08. Map showing the location of the river outlet (red triangles) and accompanying catchments (as a black line). The colour scale indicates approx. water depth from four different sources of data described in detail the text. Depth relates to the minimum water depth within 100 m x 100 m grid cells, except close to the river outlet where the individual sampled depth is shown as points. Contours mark the 2 m vertical equidistance.*

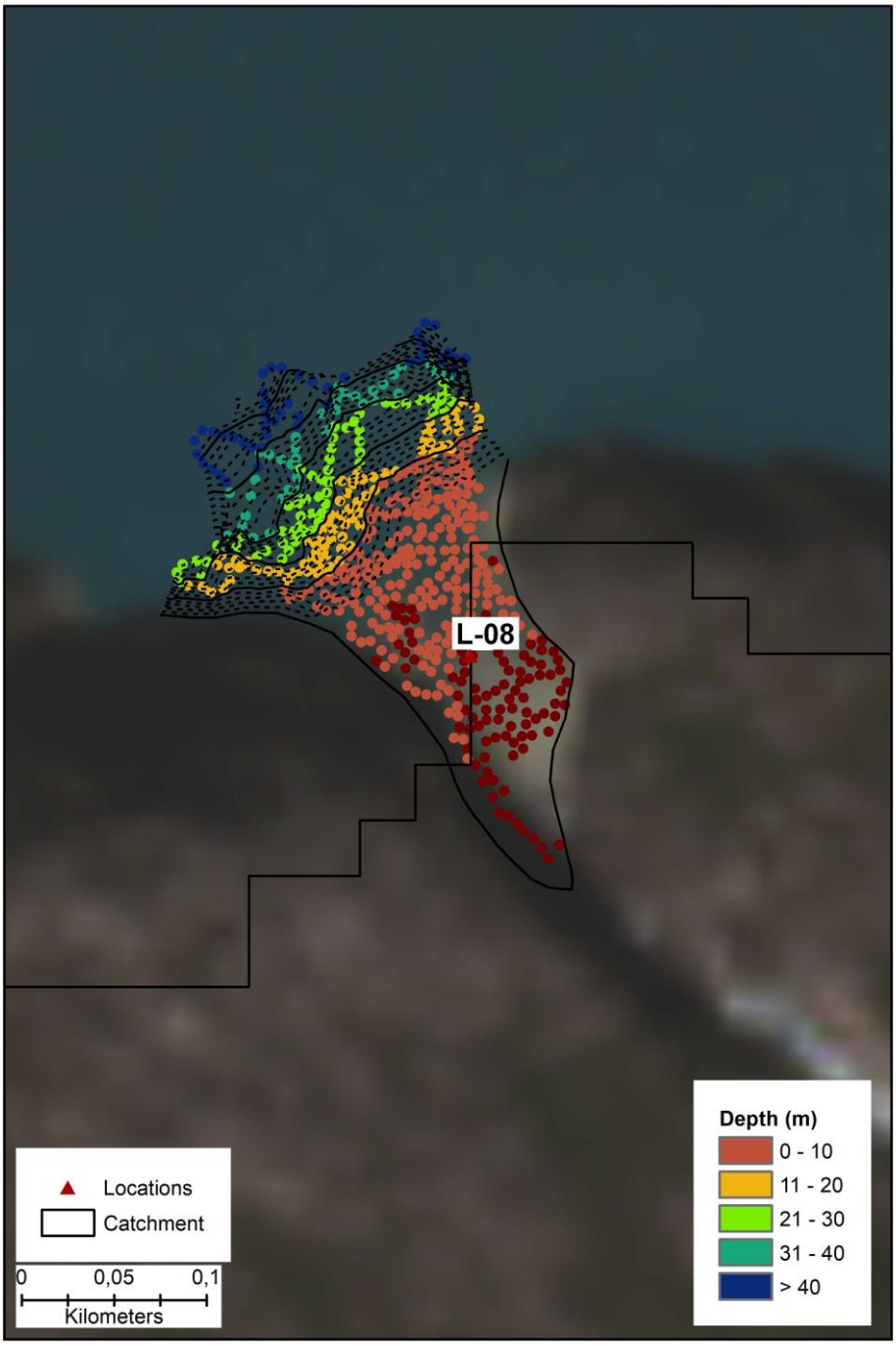

Figure 9. *Close up of Location L-08. Map showing the location of the river outlet (red triangles) and accompanying catchments (as a black line). The colour scale indicates approx. water depth from four different sources of data described in detail the text. Depth relates to the minimum water depth within 100 m x 100 m grid cells, except close to the river outlet where the individual sampled depth is shown as points. Contours mark the 2 m vertical equidistance. Note that points with dark red colour mark points above mean sea level in the intertidal zone.*

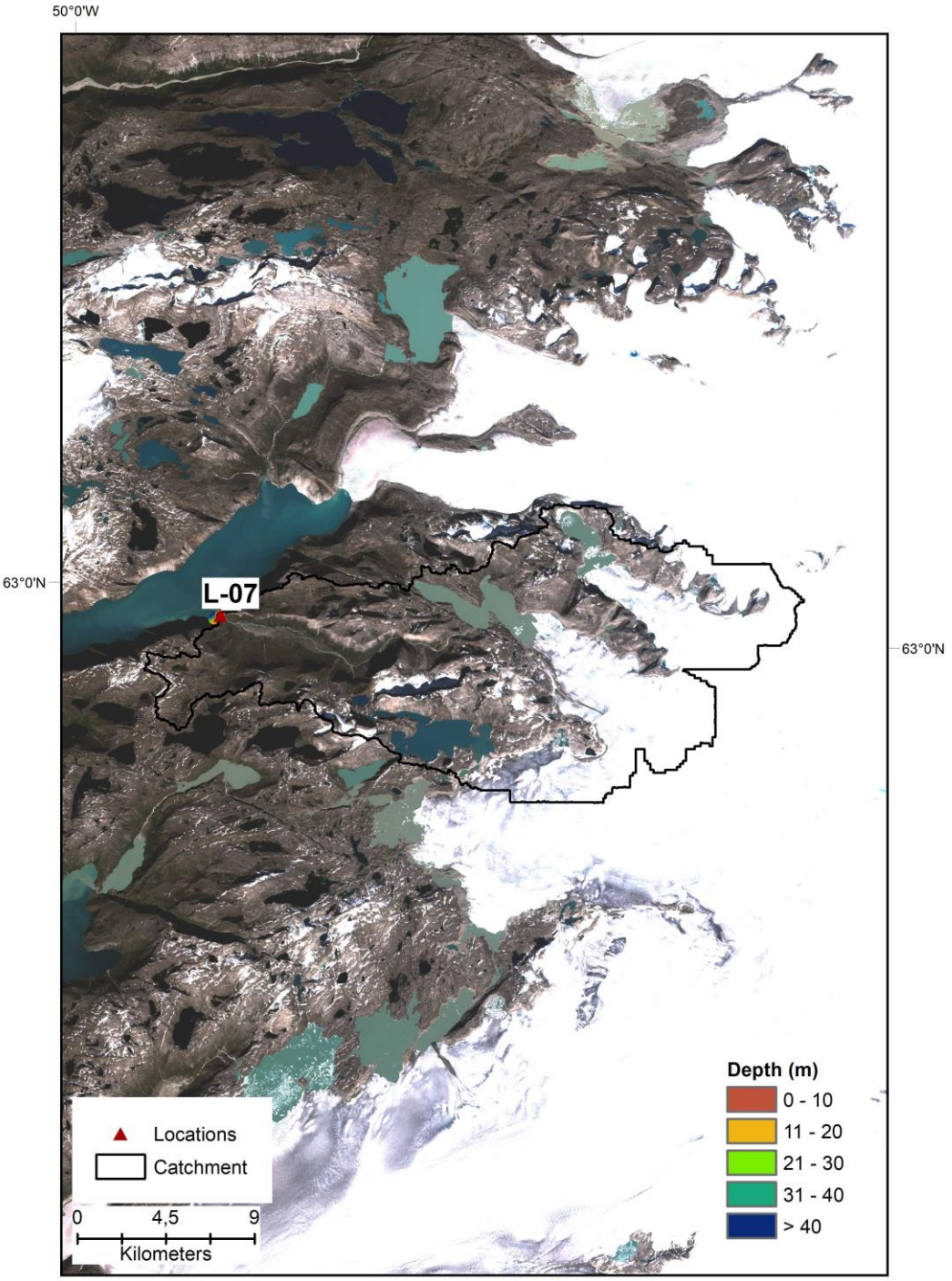

Figure 10. *Location L-07. Map showing the location of the river outlet (red triangles) and accompanying catchments (as a black line). The colour scale indicates approx. water depth from four different sources of data described in detail the text. Depth relates to the minimum water depth within 100 m x 100 m grid cells, except close to the river outlet where the individual sampled depth is shown as points. Contours mark the 2 m vertical equidistance.*

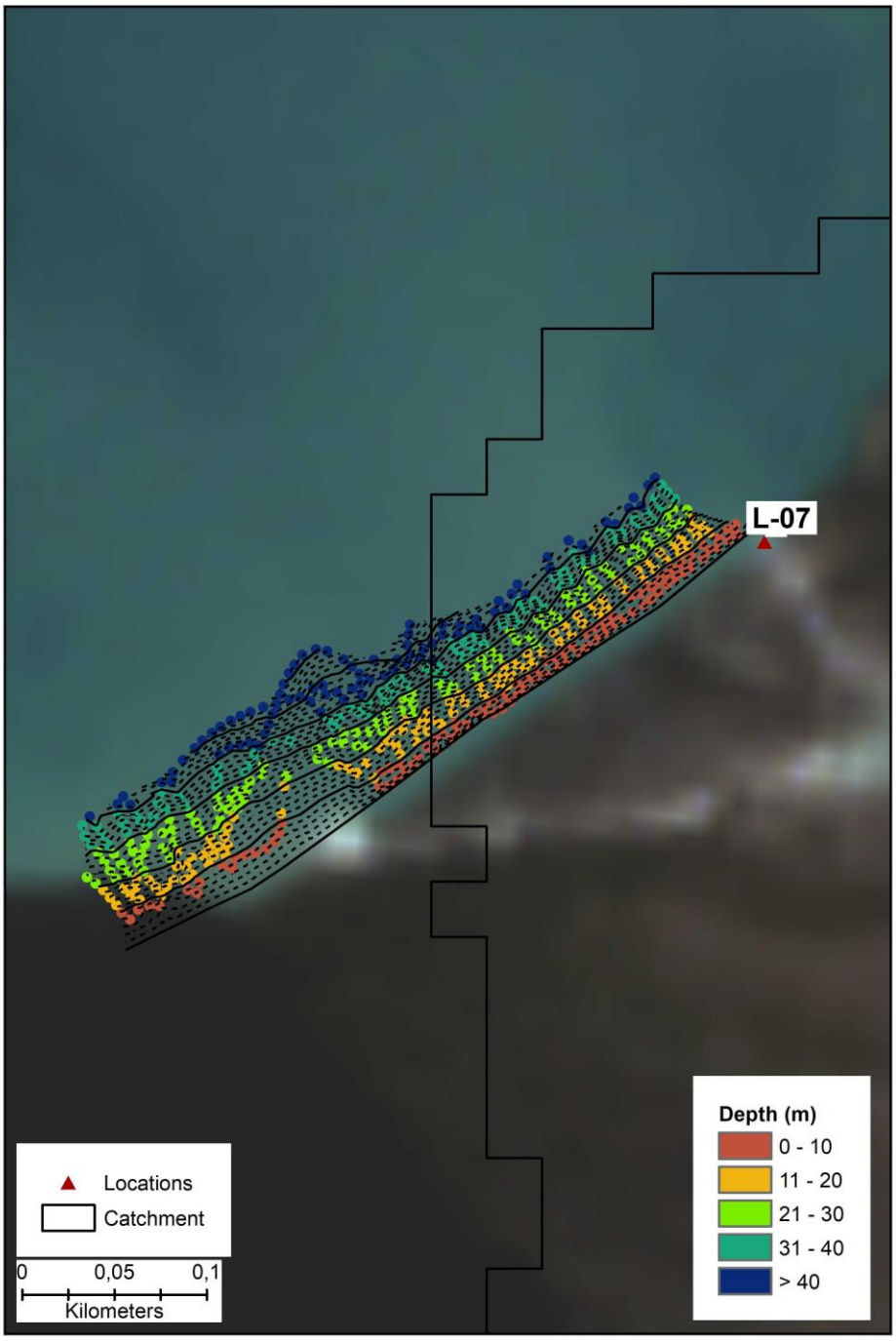

Figure 11. *Close up of Location L-07. Map showing the location of the river outlet (red triangles) and accompanying catchments (as a black line). The colour scale indicates approx. water depth from four different sources of data described in detail the text. Depth relates to the minimum water depth within 100 m x 100 m grid cells, except close to the river outlet where the individual sampled depth is shown as points. Contours mark the 2 m vertical equidistance.*

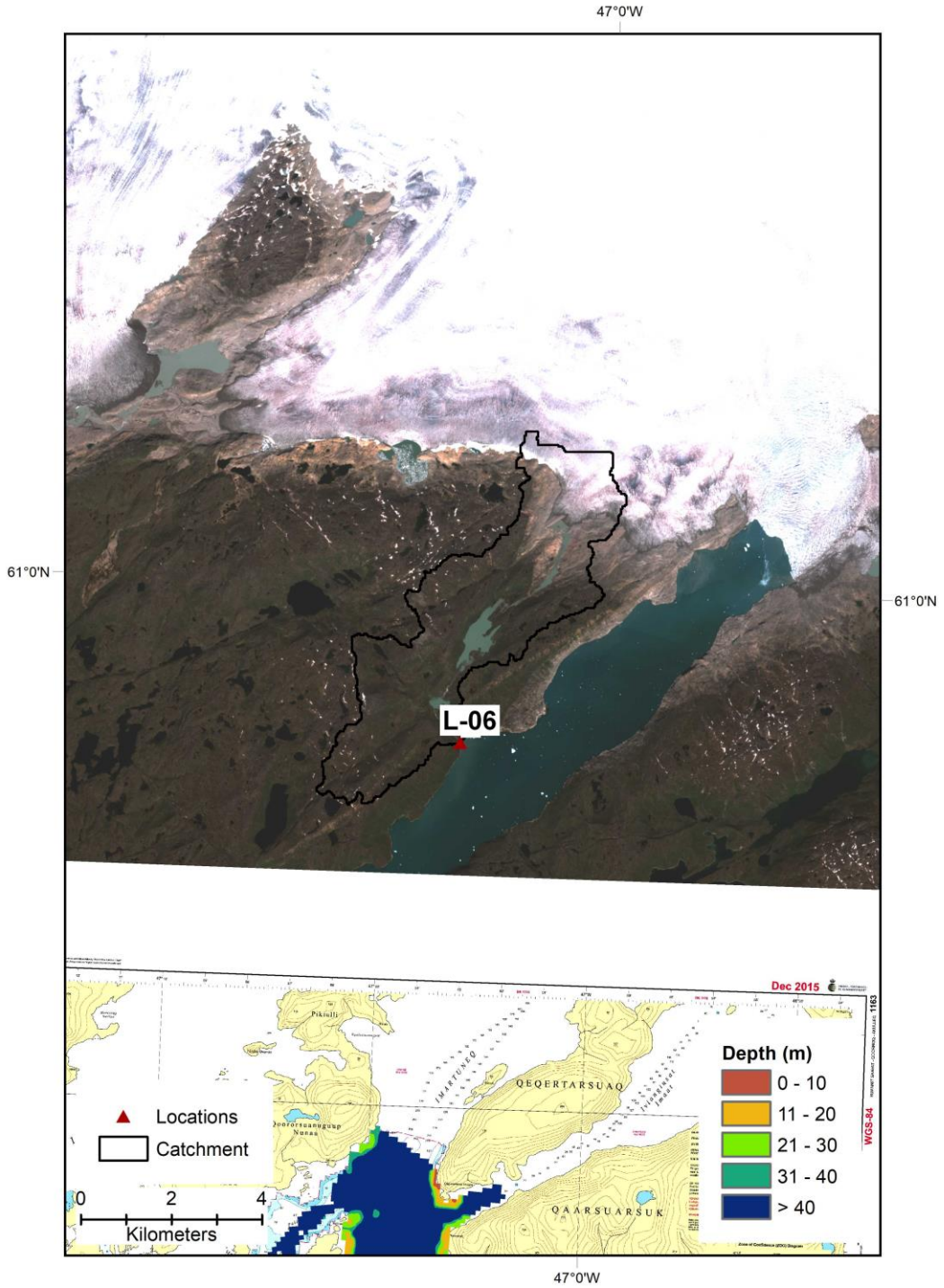

Figure 12. *Location L-06. Map showing the location of the river outlet (red triangles) and accompanying catchments (as a black line). The colour scale indicates approx. water depth from four different sources of data described in detail the text. Depth relates to the minimum water depth within 100 m x 100 m grid cells, except close to the river outlet where the individual sampled depth is shown as points. Contours mark the 2 m vertical equidistance.*

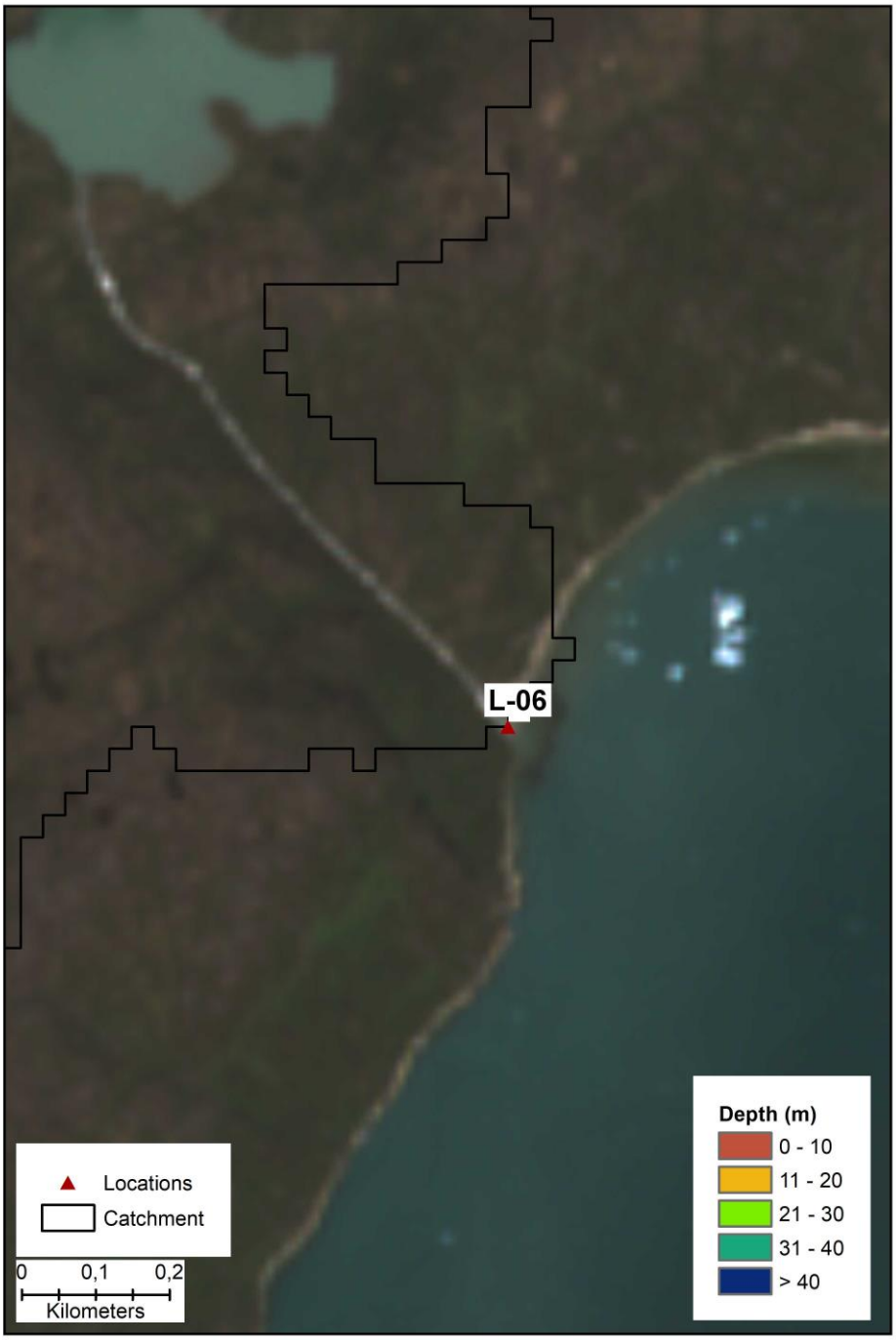

Figure 13. *Close up of Location L-06. Map showing the location of the river outlet (red triangles) and accompanying catchments (as a black line). The colour scale indicates approx. water depth from four different sources of data described in detail the text. Depth relates to the minimum water depth within 100 m x 100 m grid cells, except close to the river outlet where the individual sampled depth is shown as points. Contours mark the 2 m vertical equidistance.*

4.3 River slope

Around Greenland, water flows to the ocean via different size rivers and streams influenced by the surrounding topography. This implies that water will discharge through settings ranging from steep waterfalls to low gradient, almost flat, river outlets. In the latter case, the setting may likely be influenced by tidewater induced estuarine circulation, causing surface ocean water to impact the freshwater discharge from the river. The slope is defined by the change in elevation (the vertical) over a known stretch (the horizontal), and thus has a unit of m elevation change per m (m/m).

The slope of the individual river outlets is computed in a two-step sequence, where we first derive the horizontal stretch of the river we want to assess, and secondly, use a digital elevation model (DEM) to provide elevation differences between the start- and end-points of the desired stretch.

The horizontal stretch is obtained from manually digitizing the lowermost 500 m from the ocean/river-interface and upstream following the river configuration. In some cases, a proglacial lake is present before reaching the 500 m cutoff, and here, we have used the outflow point of the lake instead of the 500 m.

Subsequently, we extract surface elevations from the start- and end-points. The surface elevation is described using a digital elevation model (DEM), where available data is homogenized to a common fixed grid (a raster map) and each grid cell (square) is assigned a certain elevation. Here the “Greenland Ice Mapping Project” (GIMP) DEM is used [*Howat et al.*, 2014]. The DEM is comprised of different remote sensing dataset and is posted with a 30 m x 30 m resolution using the vertical datum WGS84.

Each outlet is given a score according to Table 2.

Site	Score	Criteria
L-06	1	> 0.100 m/m
L-07	2	0.050 – 0.100 m/m
L-08	2	0.050 – 0.100 m/m
L-09	1	> 0.100 m/m
L-10	1	> 0.100 m/m

Table 2. *Score based on average river slope over the lowermost 500 m of the river.*

In addition to the slope criteria, we also generate elevation contour lines from the GIMP-DEM to use during the manual screen-phase, as these provide valuable information about the topography of a given location.

5. Glaciological analysis

Knowledge of the glaciological conditions and how these may change over time is a precondition for assessing potential locations. This includes estimating the associated catchment and the ice cover within each catchment and its age, while also paying attention to potential hazards from lake outbursts.

5.1 Catchment delineation and change risk assessment

Delineating hydrological catchments in ice-covered regions is complicated by the drainage system of the ice, which is both internal and at the base of the ice, and further changes character throughout the season. For this assessment, we have employed a simplified approach in which the basal drainage system of the ice is assumed to have an internal pressure balancing the pressure exerted by the overhead ice.

A catchment represents the area which contributes to river runoff. This implies that water originating from either melting of ice or falling as precipitation anywhere within the catchments will make its way to the river outlet and contribute to the runoff (Figure 14).

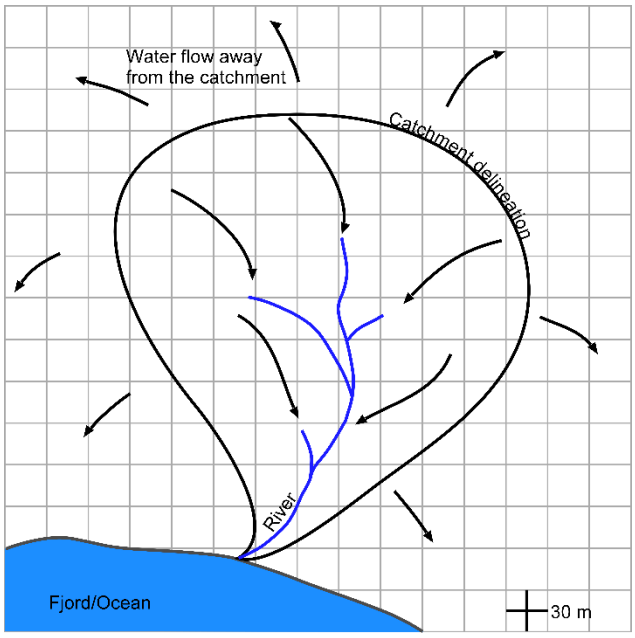

Figure 14. Illustration of catchment delineation. Water originating from either melting of ice or falling as precipitation anywhere within the catchments contribute to the river runoff and ultimately ends in the fjord.

The catchment delineation is generated from quantifying the surface gradient of the individual grid cells to determine the flow direction. Subsequently the adjoining grid cells where water will flow from one grid cell to another is summarized and ultimately provide the catchment delineation for each river or stream outlet.

Catchment delineation for individual streams have been generated for all of Greenland using a 30 m x 30 m version of the "Greenland Ice Mapping Project" (GIMP) DEM [*Howat et al.*, 2014]. This resulted in a total of 868,947 individual catchments throughout Greenland, of which 256,461 covered southwest Greenland. An initial threshold of only assessing catchments larger than 20 km^2 yielded 509, and of those only 281 intersected with local glacier ice or the ice sheet proper. These were subsequently screened to arrive at 58 locations and catchments based on the criteria outlined in Kjeldsen et al. (2019). The five locations investigated in 2018 and 2019 were chosen among these 58 locations based on their high relative score in the ranking.

5.2 Ice cover

While the Greenland Ice Sheet cover the vast majority of Greenland, many smaller local glaciers and ice caps combined, make up a large quantity of Greenland's areal coverage. Quantification of the areal ice cover was a factor in the ranking of the locations.

The ice cover is assessed using a vectorised version of the PROMICE ice mask, which is derived from manually digitized ice extent using the 1985 stereo-photogrammetric imagery [*Citterio and Ahlstrøm*, 2013]. This was manually revised using optical Sentinel-2 satellite imagery recorded during summer 2018, obtained from http://earthexplorer.usgs.gov. Additionally, ice coverage is assessed using the Randolph Glacier Inventory version 6.0 (RGI6.0) [*Pfeffer et al.*, 2014], derived from semi-automated classification scheme of available satellite imagery around year 2000. This dataset, however, only cover local glaciers and ice caps detached from the ice sheet proper.

Combining the two datasets allow quantification of the areal coverage of the ice sheet proper as well as the extent of local glaciers and ice caps within each catchment. For catchments where both datasets are represented we only use the RGI6.0 year 2000 estimate for the local glaciers and ice caps.

It should be noted that the ice coverage has changed since the time of recording the aerial- and satellite imagery in response to a changing climate. However, most changes have occurred at the lower parts of large tidewater outlet glaciers of the ice sheet proper, areas that generally do not intersect with the catchments assessed here. Further investigation of the changes is based on manual assessment using a 2m x 2m ortho-photo mosaic based on aerial vertical stereo-photogrammetric imagery recorded in 1985 [*Korsgaard et al.*, 2016] and optical Sentinel-2 satellite imagery recorded during summer 2018, obtained from http://earthexplorer.usgs.gov.

Each outlet is given a score according to Table 3. The ice coverage for each catchment is provided in Figure 15 through Figure 19. We note that on some figures there is still snow coverage, whilst the coloured areas is ice coverage according to images classification.

Site	Score	Total ice cover (km^2) – Local glaciers and ice caps	Total ice cover (km^2) – Ice sheet	Total catchment area (km^2)	Criteria for ice cover
L-06	5	0.0	2.3	20.2	0 – 4 km^2
L-07	1	8.8	91.5	279.5	> 30 km^2
L-08	2	18.6	0.0	50.0	15 – 30 km^2
L-09	4	5.0	0.0	9.4	4 – 8 km^2
L-10	3	14.9	0.0	22.2	8 – 15 km^2

Table 3. *Ice cover for local glaciers and ice caps is based on glacier outlines from the Randolph Glacier Inventory version 6.0 (RGI6.0) [Pfeffer et al., 2014], which is based on satellite imagery recorded around year 2000. Ice cover for the ice sheet proper is based on outlines from the PROMICE ice mask based on aerial imagery from year 1985, manually revised using optical Sentinel-2 satellite imagery recorded during summer 2018.*

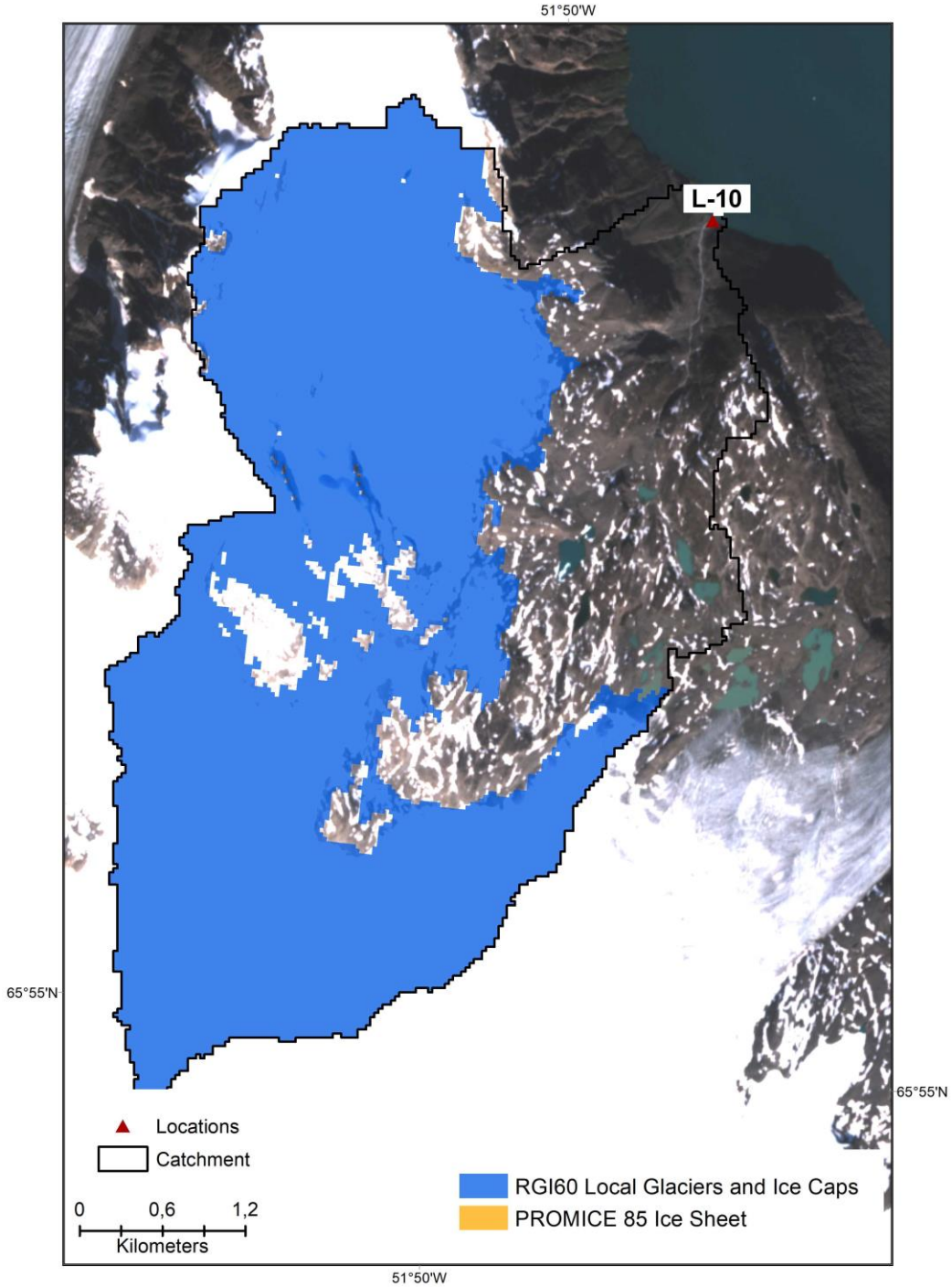

Figure 15. *Location-10. Map showing the location of the river outlet (red triangles) and accompanying catchments (as a black line) and the ice coverage according to the Randolph Glacier Inventory version 6.0 (RGI6.0) [Pfeffer et al., 2014] and the revised PROMICE ice mask described in the text. The base-map is a summer 2018 optical Sentinel-2 satellite image.*

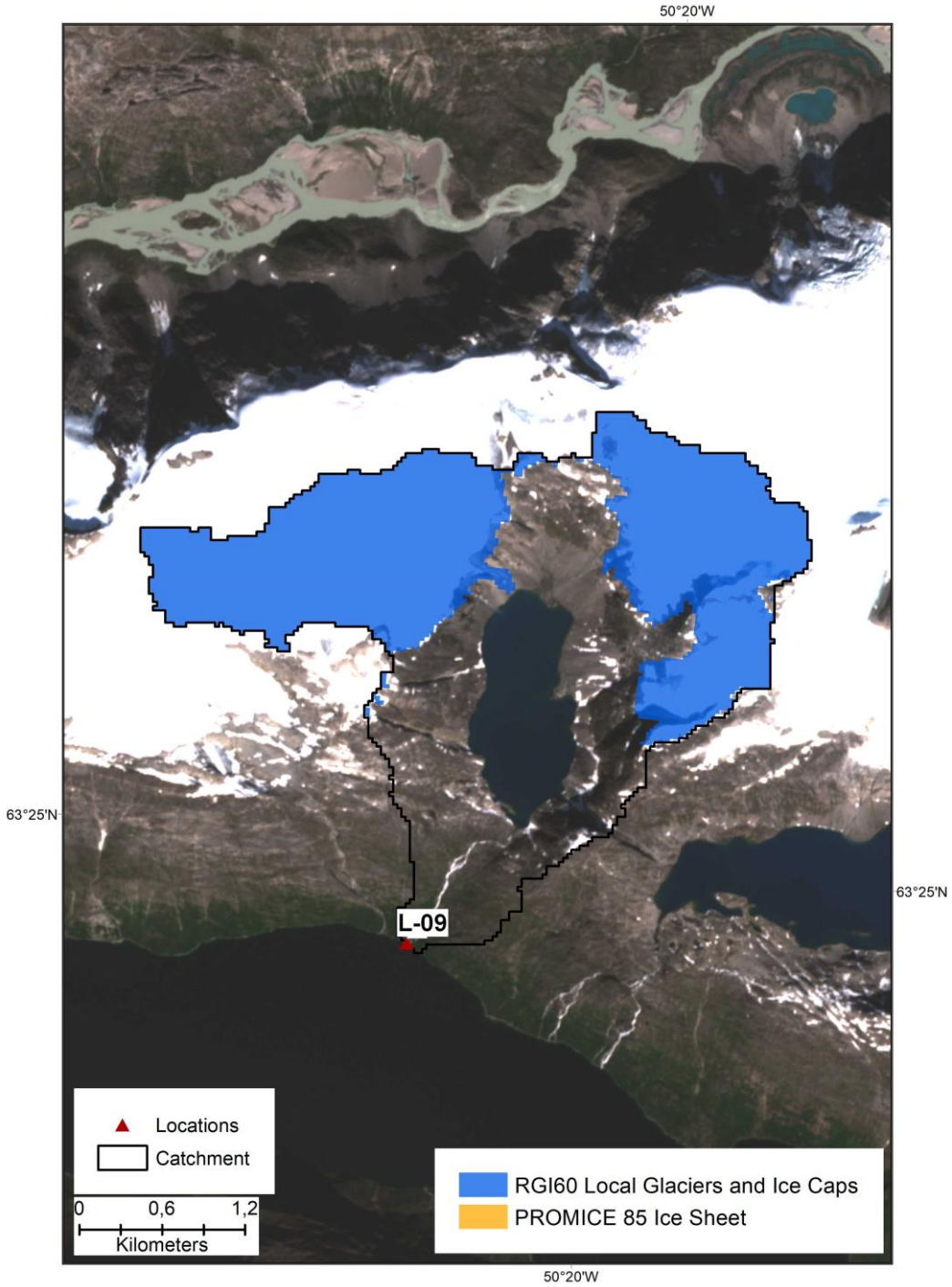

Figure 16. *Location-09. Map showing the location of the river outlet (red triangles) and accompanying catchments (as a black line) and the ice coverage according to the Randolph Glacier Inventory version 6.0 (RGI6.0) [Pfeffer et al., 2014] and the revised PROMICE ice mask described in the text. The base-map is a summer 2018 optical Sentinel-2 satellite image.*

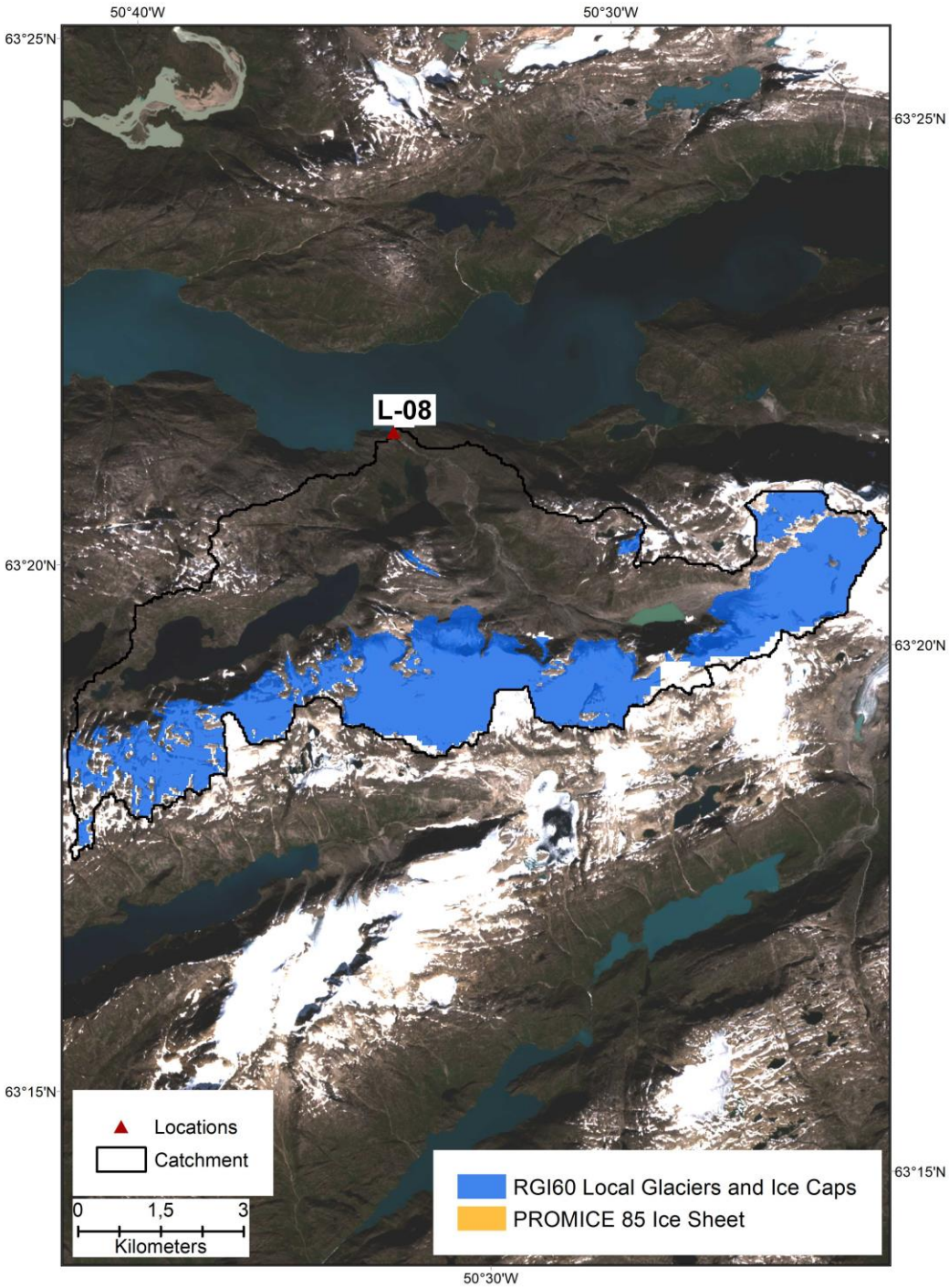

Figure 17. *Location-08. Map showing the location of the river outlet (red triangles) and accompanying catchments (as a black line) and the ice coverage according to the Randolph Glacier Inventory version 6.0 (RGI6.0) [Pfeffer et al., 2014] and the revised PROMICE ice mask described in the text. The base-map is a summer 2018 optical Sentinel-2 satellite image.*

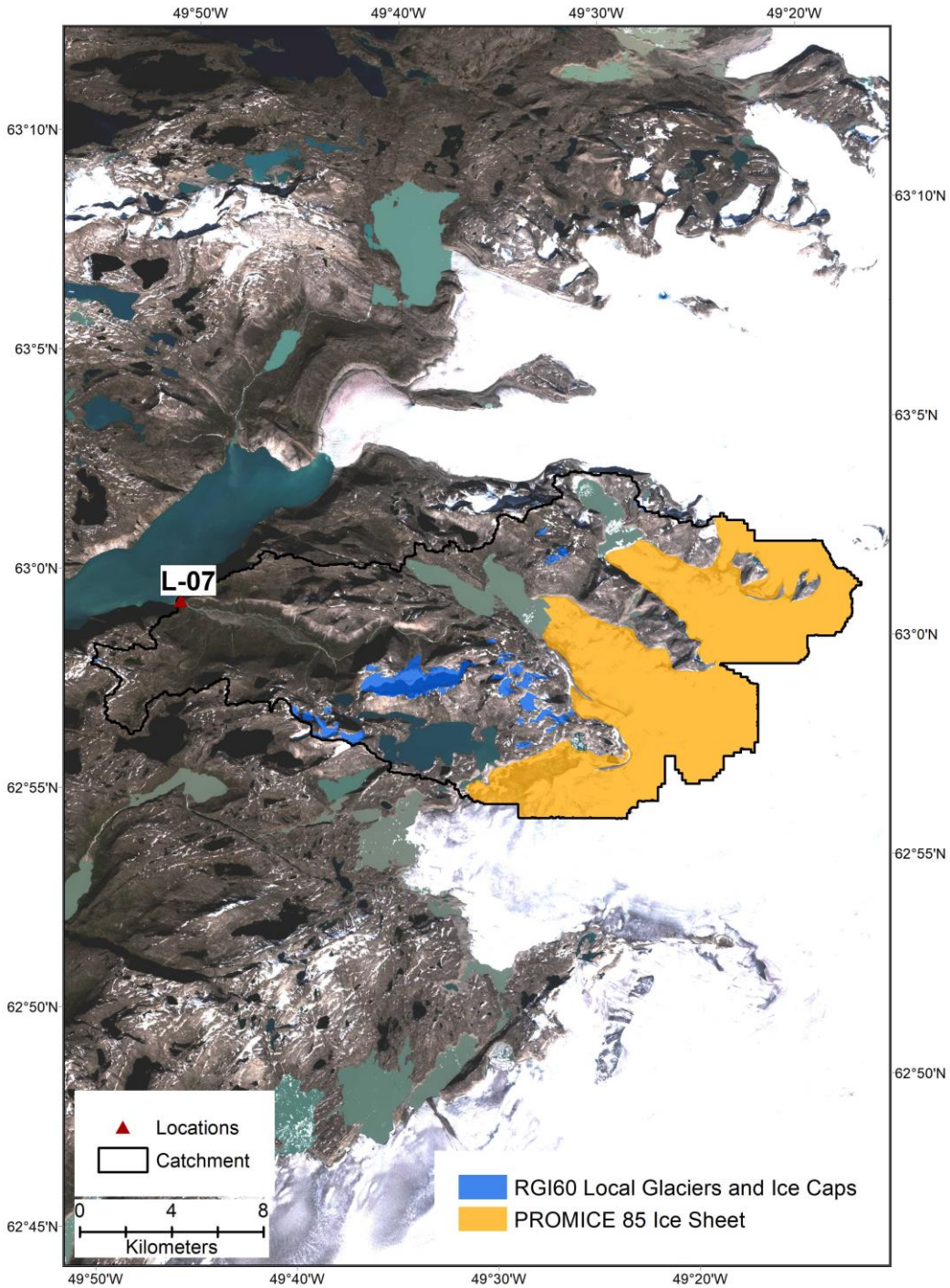

Figure 18. *Location-07. Map showing the location of the river outlet (red triangles) and accompanying catchments (as a black line) and the ice coverage according to the Randolph Glacier Inventory version 6.0 (RGI6.0) [Pfeffer et al., 2014] and the revised PROMICE ice mask described in the text. The base-map is a summer 2018 optical Sentinel-2 satellite image.*

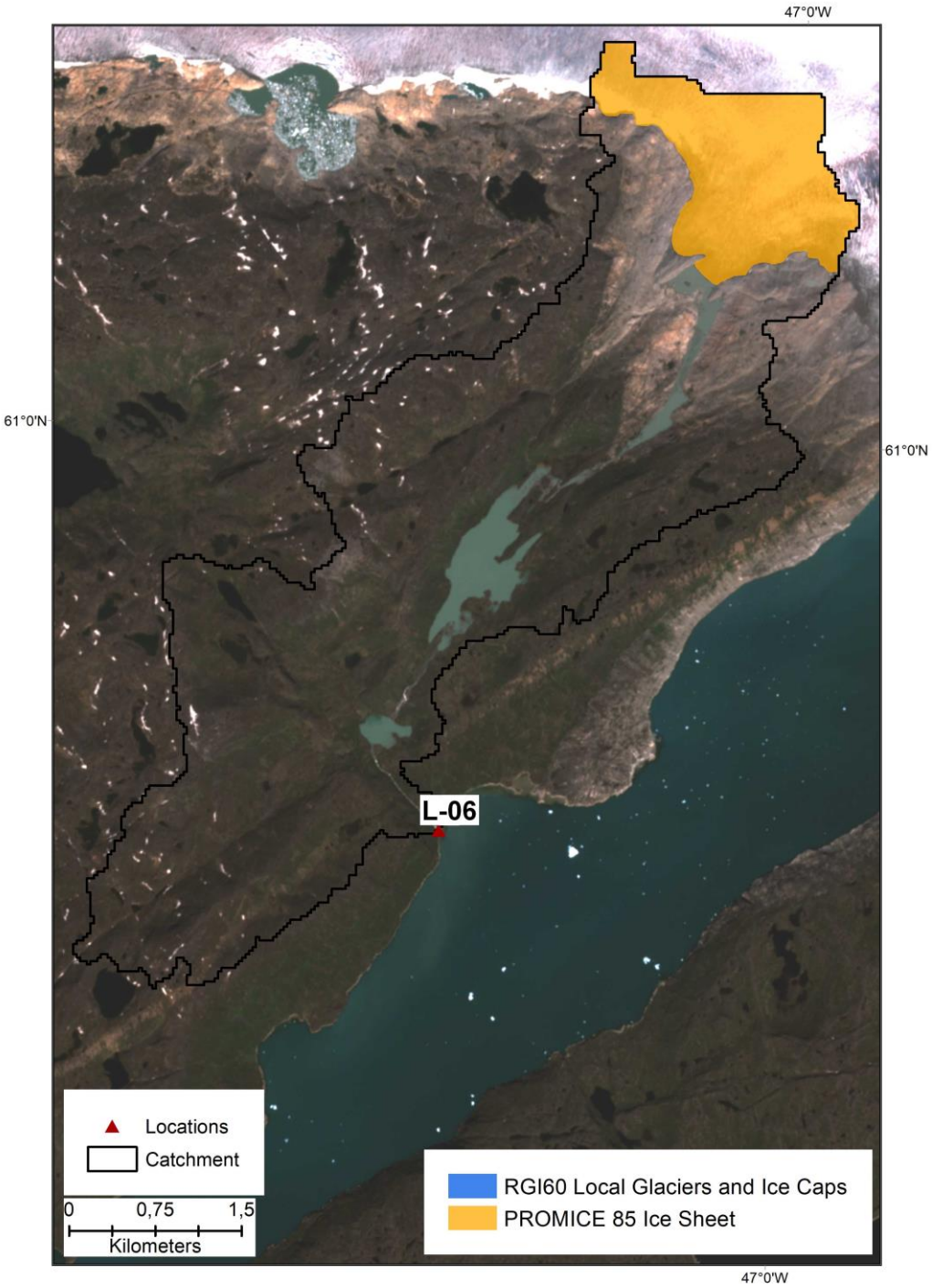

Figure 19. *Location-06. Map showing the location of the river outlet (red triangles) and accompanying catchments (as a black line) and the ice coverage according to the Randolph Glacier Inventory version 6.0 (RGI6.0) [Pfeffer et al., 2014] and the revised PROMICE ice mask described in the text. The base-map is a summer 2018 optical Sentinel-2 satellite image.*

5.3 Risk assessment of glacial lake outburst floods

A common feature of catchments adjoining the Greenland Ice Sheet is glacial lake outburst floods (GLOFs), which occur when a water volume stored in an ice-dammed- or moraine-dammed lake becomes sufficient to lift the ice barrier blocking its path downstream or if the barrier is breached. Some GLOFs are known to take place from the same ice-dammed lake every few years as the lake fills up sufficiently to break through. However, the frequency of these events is changing as the ice bodies blocking the lakes are generally thinning due to a warming climate. Thus, previous knowledge may turn out to be outdated and a known GLOF-prone lake system may pose a risk to anything and anyone downstream. To accommodate this, we have assessed the risk of GLOFs at the selected locations based on the criteria and provide a score for each site as listed in Table 4.

Site	Score	Criteria
L-06	1	*No lakes by ice margin*
L-07	2	*Outburst flood not so likely. but minor lake at the ice margin*
L-08	1	*No lakes by ice margin*
L-09	1	*No lakes by ice margin*
L-10	1	*No lakes by ice margin*

Table 4. *Glacial lake outburst flood (GLOF) risk level and score for each site.*

5.4 Estimation of the age of the meltwater source ice

A significant part of the water discharge consists of ice sheet or glacier meltwater. The age of the source ice for this meltwater can be many thousands of years and depends partly on local conditions, but is generally governed by upstream conditions. The left part of Figure 20 shows a cross section of an ice sheet, from surface to bedrock. Two trajectories illustrate possible particle paths through the ice sheet for an ice crystal, originally falling as snow, depending on where it originates on the ice surface. It illustrates that the higher on the ice sheet the snow fell in the accumulation zone, the deeper the trajectory of the ice crystal, and subsequently, the closer to the ice margin the reappearance in the ablation zone. The accumulation zone is the only region on an ice sheet or glacier, where the mass balance is positive, i.e. more snow is deposited than what melts or blows away, whereas the opposite is true in the ablation zone, where the mass balance is negative, i.e. more mass is removed than added. This implies that layer after layer of snow is buried in the accumulation zone every year, while in the ablation zone they reappear. If there was no melting at the base of the ice sheet and the internal ice layers never folded, it would in principle be possible to make ’horizontal’ ice cores along the surface of the ice margin, with the oldest ice closest to the margin as illustrated in the right side of Figure 20. The age of the ice at the margin is thus determined by the distance and pace of the ice movement towards the margin. This implies that under the right circumstances, it is possible to find extremely old ice at the ice sheet margin, as shown in e.g. Reeh et al. (2002).

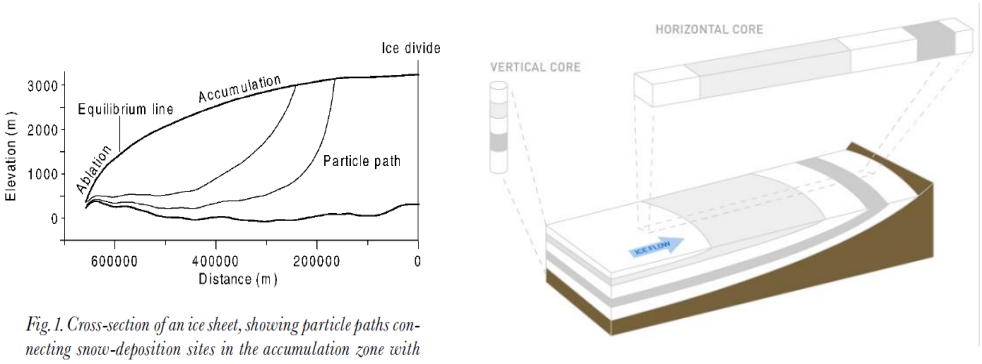

Fig. 1. Cross-section of an ice sheet, showing particle paths connecting snow-deposition sites in the accumulation zone with locations where the ice resurfaces in the ablation zone.

Figure 20. *Two figures, illustrating why old ice can be expected at the ice sheet margin. Left: Reeh et al. (2002). Right: figure from www.niwa.co.nz.*

5.4.1 Ice-dynamic model setup

To estimate the age of the ice at the ice sheet margin, we have employed the ice-dynamic model PISM (Parallel Ice Sheet Model), which is a three-dimensional, thermo-mechanical coupled model (Bueler and Brown, 2009; Winkelmann et al., 2011; Aschwanden et al, 2012). The model is developed at the University of Alaska and the Potsdam Institute for Climate Impact Research. PISM makes use of a simplified description of ice-dynamics, combining the so-called 'shallow-ice' and 'shallow-shelf' approximations, which makes it possible to study the flow of large ice masses like the Greenland Ice Sheet, over long time scales (tens of thousands of years), as those of interest here. The model has an 'age-tracking' method, thereby keeping track of the age of the ice, a method we employ to estimate the age of the ice at the margin.

As input to the model, we have used present-day topography forced with present-day climate (surface mass balance and air temperature; Ettema *et al.* 2009). The model covers the entire Greenland Ice Sheet with a spatial resolution of 10 km. All model experiments have been conducted over a 100,000 year period of constant climate, reaching a steady state during this time. Additionally, model experiments at 20 km spatial resolution with only the 'shallow ice' approximation have been conducted to test the robustness of the results. These sensitivity model runs show the same results as the main model experiments on the scale examined here.

Present-day surface mass balance (precipitation - runoff) is shown in Figure 21, where blue-ish colours illustrate regions with net melting (the ablation zone), while yellow/green-ish colours shows the accumulation zone, where snowfall exceeds melt. The ablation zone is generally quite narrow, but widens in some regions, like western Greenland, where it is more likely to find ancient ice at the surface due to the long distance between the ice margin and ice divide in the interior. Contrary to this, in southern Greenland, it is expected that ice at the margin is typically younger and that the older ice resurfaces in a narrower region as the distance to the ice divide is short, the accumulation rate is high, and the ablation zone is narrow.

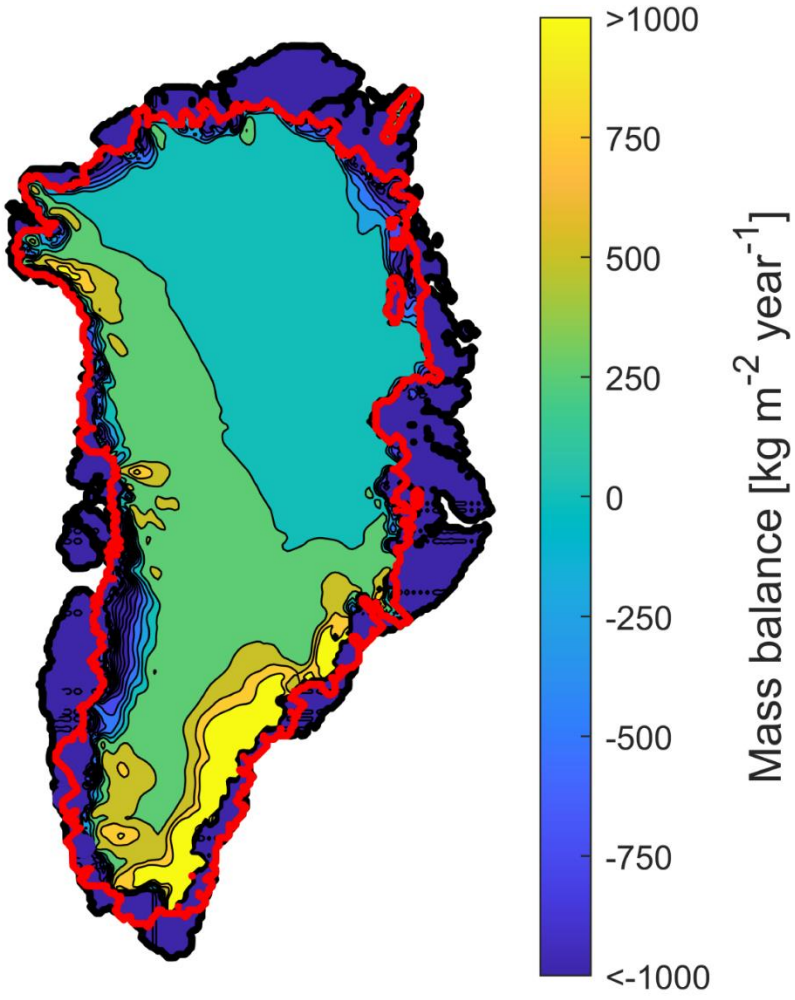

Figure 21. *Present-day surface mass balance from Ettema et al. (2009). The red line indicates the extent of the ice in the model following spin-up over 100,000 years. The black line separates land/ice from ocean. The region between the red and the black line is thus ice-free land in the model.*

5.4.2 Estimated age of the ice

During the spin-up phase, the model is set to run over 100,000 years, forced with present-day climate, to reach a steady state. The resulting configuration of the modelled ice sheet is a somewhat larger extent and volume than the actual present-day Greenland Ice Sheet. This is a consequence of using present-day climate to force the model, as the present-day ice sheet is not in balance with present-day climate, as well as the choice of 10 km spatial resolution. More detail could be resolved if running the model at higher spatial resolution, both with respect to the surface mass balance, where it may play an important role due to the narrow ablation zone, and in relation to the basal topography, where smaller outlet glaciers would become apparent. However, running the model at a higher spatial resolution significantly increases the computational cost, and the current model setup is well suited to estimate the age of the ice even if topographical detail is not at the highest spatial resolution.

While the model experiments have been conducted prescribing a 100,000 years of constant climate, the climate has of course not been constant over this period. During the last ice age, which terminated around 11,700 years ago, it was of course much colder than today and accumulation was around half of the present-day value. These conditions influence the flow of the ice and has an impact on the estimation of the age of the ice. For this reason, we distinguish between either ice-age ice (i.e. generally older than 11,700 years) or the younger Holocene ice (Holocene: Geological era covering 11,700 years ago to present).

The modelled age of the ice appearing on the surface is shown in Figure 22, while Figure 23 shows two examples of cross sections, where layers of various age can be traced in the ice sheet.

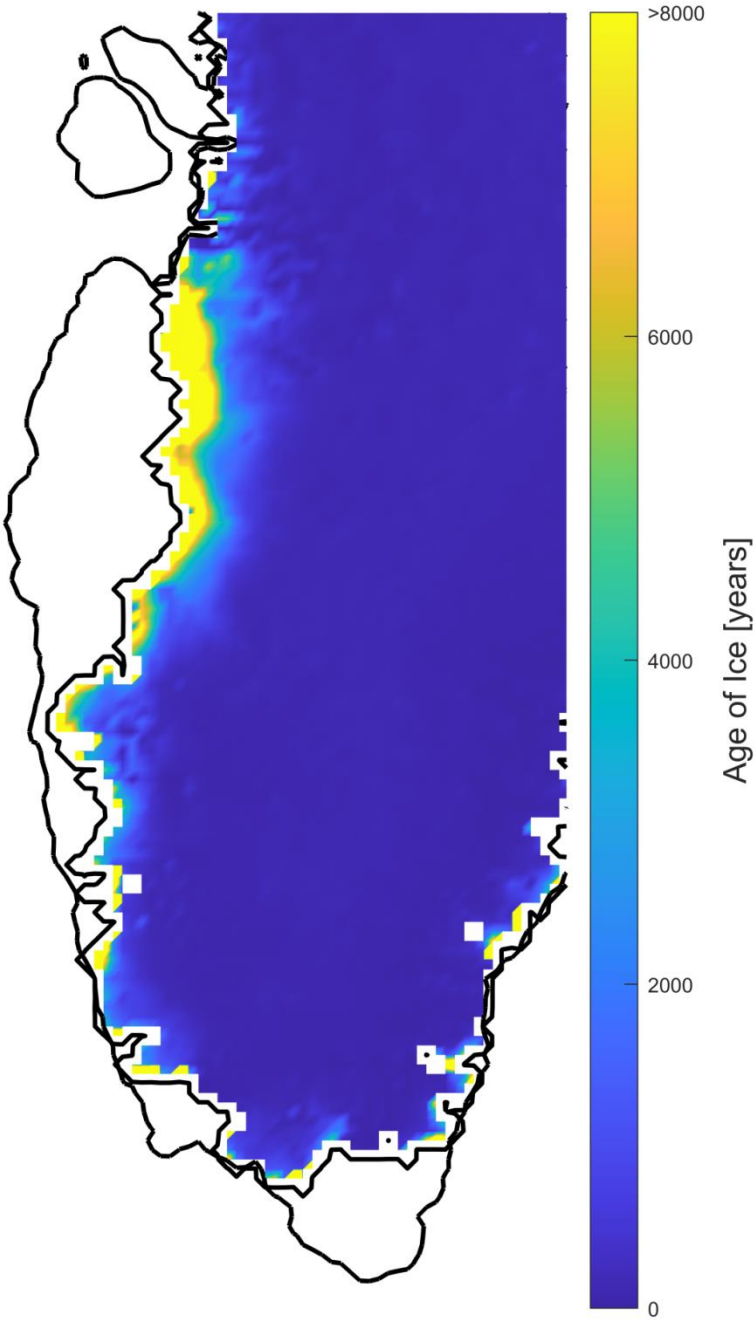

Figure 22. *Estimated age of the ice at the surface based on the model run.*

In the region with the broad yellow ablation zone in Figure 22, the age at the surface of the ice exceeds 8,000 years. However, the narrow, yellow areas/dots in the southern region are artefacts from the ice modelling in combination with the contouring method, and thus not a real indication of pre-Holocene ice surfacing.

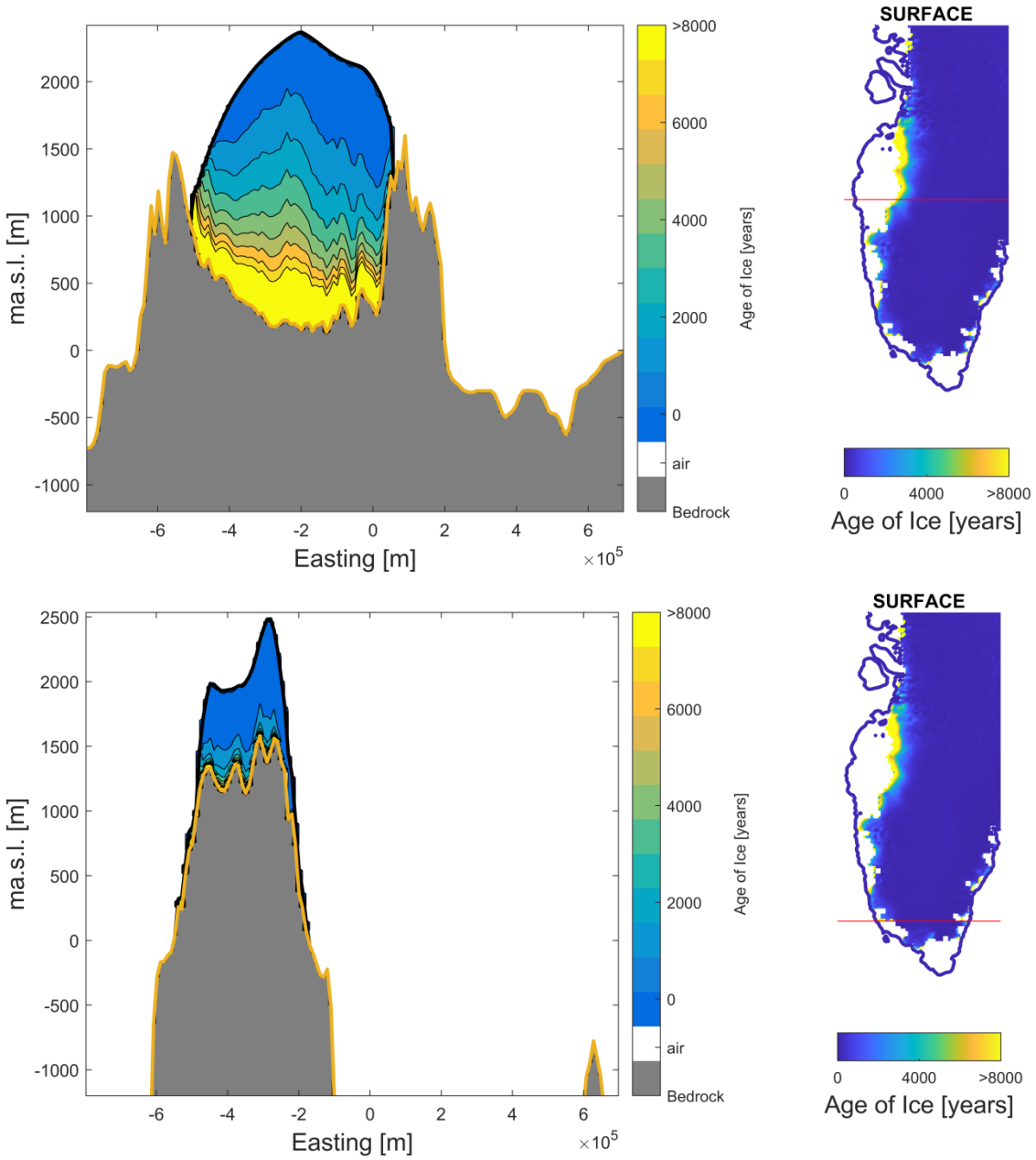

Figure 23. *Top left panel: cross section of the ice sheet in southern West Greenland showing the age of the ice at depth along the thin, red line shown in top right panel. Bottom left panel: cross section of the ice sheet in the extreme South Greenland showing the age of the ice at depth along the thin, red line shown in bottom right panel. Notice the different scale of the x- and y-axis, distorting the relationship between the width and the height of the ice sheet.*

Our results indicate that ice from the last ice age can be found at the surface of the ice margin in a region between Disko Bay and south of Kangerlussuaq in Southwest Greenland. This is supported by oxygen isotope measurements from a few sites in the region (Reeh et al., 2002). In South Greenland, the ice is mainly of Holocene age. Even though the ice extent in our simulation is larger than actual present-day extent, it is still possible to conclude that the ice is of Holocene origin. This also matches an earlier investigation by

Mayer et al. (2003), who found ice of an age of 5-6,000 years at two locations in South Greenland.

For the locations that do not receive meltwater from the Greenland Ice Sheet, but rather from local glaciers and ice caps, the age of the melting ice is expected to be young and most likely no older than the latter half of the Holocene. This conclusion is based on the more limited extent of the local glaciers and ice caps and their location in a maritime climate with more precipitation.

The coarse subdivision of ice into that of *late Holocene*-, *Holocene*-, or *ice-age*- ice is a consequence of the simplified model setup. A more specific age determination of ice from a particular location can be estimated by combining modelling of the ice dynamics within the individual ice catchment with oxygene isotope measurements of samples from the ice surface.

The score and estimated age of the ice within each catchment is listed in Table 5.

Table 5. *The modelled or estimated age of the ice from which the meltwater originates at the selected locations. The age has been estimated from glaciological expertise and comparison to model results of the ice sheet proper.*

Site	Score	Source	Age	From
L-06	2	Younger inland ice	Holocene	Model
L-07	2	Younger inland ice	Holocene	Model
L-08	4	Primarily from local ice cap	Late Holocene	Estimate
L-09	4	Primarily from local ice cap	Late Holocene	Estimate
L-10	4	Primarily from local ice cap	Late Holocene	Estimate

6. Meltwater abundancy

To give the best possible estimate of the runoff from the selected catchments, we utilized the results from the reconstructions of the 1900–2018 Greenland ice sheet surface mass balance using the regional climate model MAR, described in detail in Fettweis et al., 2017. The regional climate model is run over a Greenland-wide domain of 15 km resolution with daily calculations of surface runoff (amongst other values) from precipitation and melt of snow and ice. The model is driven by the ERA-interim, reanalysis data at the domain boundary (Dee et al., 2011). The monthly averages of this product is downscaled to a domain of 1 km resolution in order to resolve the topography around the ice sheet margin.

To illustrate the development of the runoff from the Greenland Ice Sheet and surrounding ice caps and glaciers over the last 35 years, we have chosen to split the climate model run into two reference periods of each 12 years. The first time period is 1980-1991 and the second time period is 2006-2017. For catchments of sufficient size, runoff was estimated using the monthly downscaled values from MAR. We have derived the annual mean values for the runoff from both periods (Table 6), as well as the monthly mean values over the period (see Figure 24).

Table 6. *The mean annual runoff modeled for two 12-year periods, with climate input data downscaled from the regional climate model grid cell nearest to the center of the catchment. "Min" and "max" values show the largest possible variability in the derived discharge arising from exchanging the center grid cell with each of the eight neighbouring grid cells in the regional climate model (all within 15 km of the center grid cell). The min-max range illustrates the impact of the spatial variability in the climate model output on the modelled discharge.*

Location	1980-1991			2006-2017		
	center	**min**	**max**	**center**	**min**	**max**
L-06	**21.9**	16.9	26.4	**21.4**	16.1	25.4
L-07	**240.8**	168.9	296.4	**291.1**	185.8	353.1
L-08	**59.6**	44.7	67.1	**73.5**	52.5	83.5
L-09	**8.7**	7.0	9.9	**10.5**	8.4	12.8
L-10	**7.9**	7.8	16.2	**14.5**	14.5	31.7
	[x 10^9 L]	[x 10^9 L]	[x 10^9 L]	[x 10^9 L]	[x 10^9 L]	[x 10^9 L]

Some of the selected catchments are too small to be properly resolved in the regional climate model. For these small catchments, we adopt a different approach. Since all catchments in consideration are partly glaciated, we have chosen to use a well-established model for calculating both melt and runoff in glaciated mountainous areas: The Distributed Enhanced Temperature-Index Model (from hereon called meltmodel) (Hock, 1999). The meltmodel requires temperature and precipitation as a minimum input. The model considers the climate input as a point measurement, and distributes the values using topographical lapse-rates. Thus model resolution can be as high as the digital terrain model used, in this case the Greenland Ice sheet Mapping Project (Howat et al., 2014) DEM with a resolution of 30 m. As input for the meltmodel we use daily temperature and precipitation outputs from the daily MAR product which has a resolution of 15 km. The meltmodel is set up with

values according to literature (Janssens and Huybrechts, 2000; Hock, 1999). Temperature and precipitation is extracted from the grid cell in MAR that covers the center of the catchment. Uncertainties in the calculated runoff values, due to input data is tested by running the meltmodel with input values from the eight neighboring grid cells in MAR. Thus, the given minimum and maximum values in Table 6 represents how calculated runoff can change based on input climate alone.

The difference in runoff between the two periods (Table 6 and Figure 24) are due to changes in weather and climate conditions. Model results for all catchments show an increase in the mean annual meltwater runoff from the first period to the second period (Figure 24 and Figure 25). Furthermore, the largest change is seen in the summertime (June-August, Figure 24 and Figure 25). The general increase in ice sheet runoff from the model is a direct consequence of the larger amount of energy received from an increasingly warmer climate.

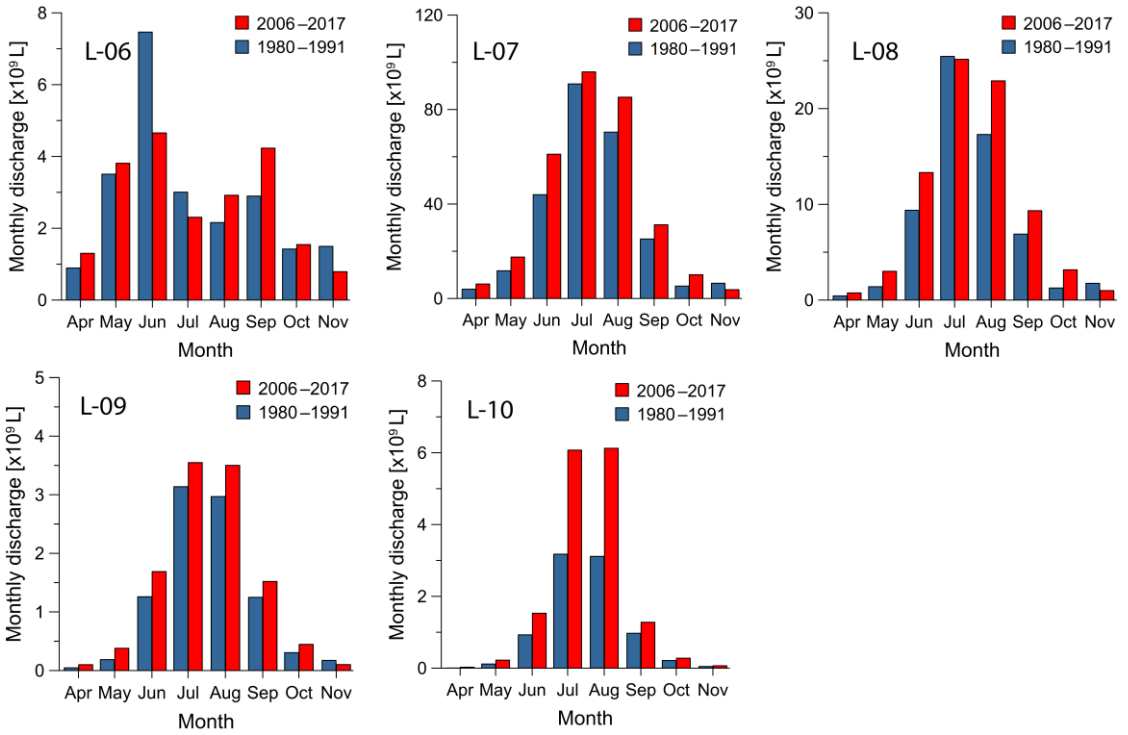

Figure 24. *The total monthly discharge given in litres at each of the catchments, calculated as mean values over two separate periods, 1980-1991 and 2006-2017, respectively.*

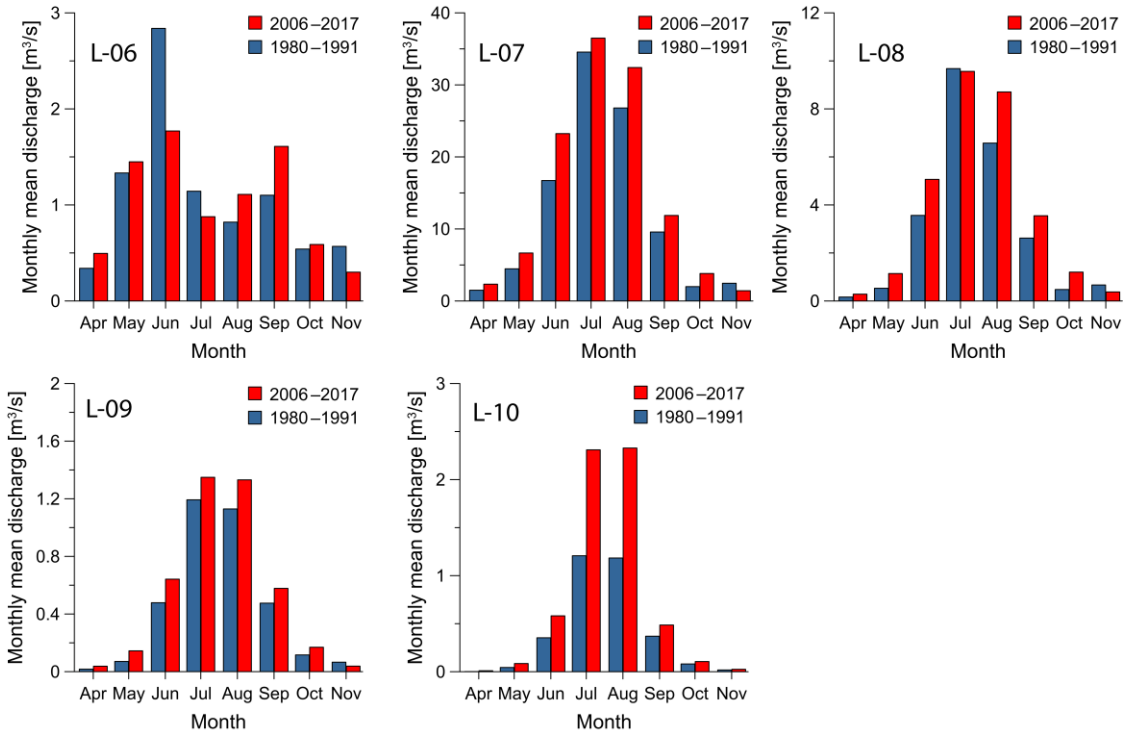

Figure 25. *The monthly discharge given in cubic metres per second at each of the catchments, calculated as the monthly mean over two separate periods, 1980-1991 and 2006-2017, respectively.*

7. Water quality analysis

7.1 Analysis program and sampling methodology

Water samples were retrieved from the five locations during four field campaigns (Table 7). The four field campaigns were carried out in June 2018, September 2018, June 2019 and September 2019.

Table 7. *GPS-coordinates and dates for water sampling for chemical, sediment and microbiological parameters for new locations visited in 2018 and 2019.*

Location	N	W	June sampling date	Sep. sampling date
L-06	60°58.217	47°03.184	11/6-2018	10/9-2018
L-07	62°59.448	49°48.435	14/6-2019	9/9-2018
L-08	63°21.490	50°33.557	12/6-2019	6/9-2019
L-09	63°24.644	50°21.635	13/6-2019	7/9-2019
L-10	65°58.232	51°48.442	17/6-2019	10/9-2019

Water sampling was as far as possible conducted where the water was well-mixed and where no animal droppings were visible on shore. When possible, samples were taken a few metres from the shore of the river. The person sampling wore nitrile gloves, which were disinfected with ethanol before sampling the water.

Samples for chemical analyses were kept in various plastic and glass bottles depending on the sample type (see Table 8 for overview). Samples for analysis of metals, cyanobacterial toxins (microcystins), anions and cations were initially taken in a 250-mL sterilized and acid washed glass bottle, which was stored for 1-2 hours before the contents were divided as partial samples into the final analysis bottles. For analysis of trace metals, nitric acid was added to the analysis bottle prior to use. Since nitric acid may extract metal from the suspended sediment, trace metals were analyzed in unfiltered as well as filtered (Q-max PES 0.45 µm) samples. For anions, cations and alkalinity, a 20-mL sample was filtered through a Q-max PES 0.45 µm filter and transferred to a plastic vial.

Samples for bacterial counts were collected in sterile 50-mL centrifuge tubes, by opening the tubes 10-20 cm below the water surface to avoid any surface film. This sample was used for bacterial counts of undiluted sample. Additionally, total plate counts (heterotrophic colony forming unit, CFU) were done for 10-fold diluted samples. The dilutions were prepared by using filter-sterilized water (0.2 µm cellulose acetate filters) from the same streams. Samples were transfered to petrifilms onboard the ship by using sterile pipette tips, nitrile gloves disinfected with alcohol, and a table disinfected with alcohol.

Table 8. *Analytical program for chemical, sediment and microbiological parameters.*

Parameter	Type of analysis	Place of analysis	Container	Comment
pH	Electrode	On-site	n/a	
Conductivity	Electrode	On-site	n/a	
Anions[1] + cations[2]	Ion chromatograph	GEUS	20 mL plastic	Filtered, kept cold
Trace metals[3]	DS/EN ISO 17294m:2016 ICP-MS	Eurofins	30 mL plastic	Acid conservation, filtered and unfiltered
Radioactivity[4]	ISO 10704+13168:2015	Eurofins	250 mL plastic	Unfiltered
Microcystins[a)]	ISO 20179 mod. LC-MS/MS	Eurofins	100 mL glass	Added thiosulfate, kept cold
Sediment[5]	Gravimetric + Malvern	GEUS	1 L plastic	Four replicates
Total CFU	3M Petrifilm Aqua 5 x 1 mL	On-boat	22°C incubator 68h	Undiluted + 10-fold diluted
Thermotolerant CFU[b)]	3M Petrifilm Aqua 5 x 1 mL	On-boat	36°C incubator 44h	Undiluted
Coliform bacteria	3M Petrifilm Aqua 5 x 1 mL	On-boat	36°C incubator 21h	Undiluted
Enterobacteriaceae	3M Petrifilm Aqua 5 x 1 mL	On-boat	36°C incubator 21h	Undiluted

[a)]Analyzed only in September 2018.

[b)]Method developed for total CFU but adapted to thermotolerant CFU.

[1]Fluoride, chloride, bromide, sulfate, nitrate, phosphate.

[2]Sodium, potassium, calcium, magnesium.

[3]Aluminum, Antimony, Arsenic, Barium, Lead, Boron, Cadmium, Chromium, Cobalt, Copper, Mercury, Nickel, Selenium, Zink. See Appendix A for full list of trace metals that are included in one or more guideline.

[4]Total indicative dosis, total alpha-activity, total beta-activity, tritium activity

[5]Concentration and grain size distribution

7.2 Inorganic parameters including selected trace metals and radioactivity

Inorganic water constituents cover a wide range of elements and minerals, including nutrients, salts and metals (including heavy metals which are metals with larger density than iron). Especially heavy metals can be of concern for drinking water quality and guideline limits exist for several heavy metals as well as for some of the major inorganic constituents (Appendix A). Heavy metals have not previously been reported in problematic concentrations in Greenlandic streams, but it is known that the local geology varies with some hotspots of high metal concentrations in the bedrocks occurring especially in Southern Greenland. The geology below the Inland Ice is basically unknown and analysis of a number of inorganic parameters are therefore included to characterize the water quality of the different streams.

Results from the analyses are reported in Table 9 along with the corresponding quality requirements. With the exception of aluminum in *non-filtered* samples and nickel in the *non-filtered* sample from L-10 in September, none of the chemical parameters investigated exceed the current drinking water quality requirements in Greenland, Denmark, the EU or the USA, or for bottled water in Denmark and of the ICBWA (The International Council of Bottled Water Associations). The fact that aluminum-concentrations are very high in unfiltered samples is probably due to extraction of aluminum from the sediment when the acid is added for conservation. Also some of the other metals (e.g. nickel, chromium) show rather high concentrations in unfiltered samples but low when the samples are filtered. This shows that sediment needs to be removed before the water is bottled, which is actually a requirement in itself due to guideline limits for turbidity (see Section 7.4 on sediment content).

In Figure 26, two examples of relationships between metals in unfiltered samples and sediment contents of the samples are shown along with results from similar samplings at other sites. For aluminum, the relationship is quite clear, while for nickel, there is some variation. For aluminum, this indicates that the total concentration in sediment and the fraction of aluminum that is extractable with the conservation agent (HNO_3) are similar across streams. In the case of nickel (and most of the other metals), there must be differences between streams either in the total nickel concentration in the sediment or in the fraction that is extracted with HNO_3. No general seasonal pattern seems to exist.

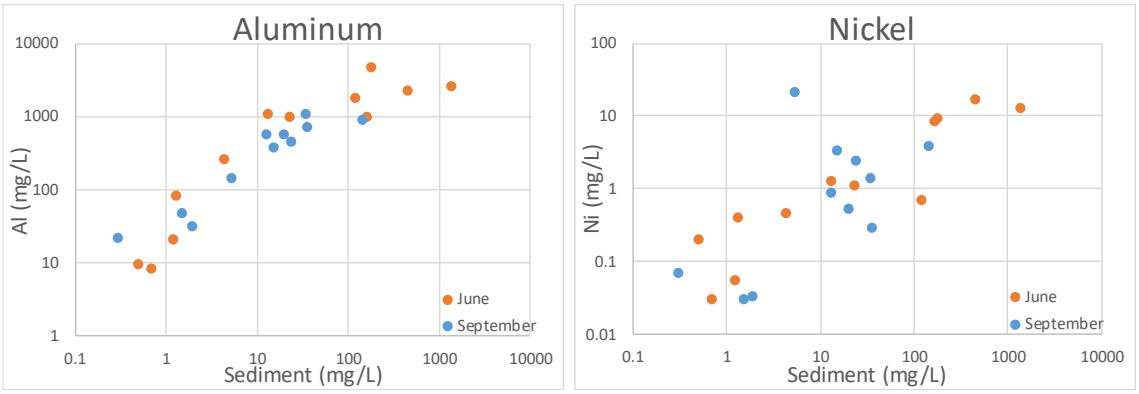

Figure 26. *Relationships between aluminum (left) and nickel (right) and sediment content of unfiltered samples. Note the logarithmic scales.*

Table 9. *Content of inorganic ions and trace metals at the streams visited in 2018 and 2019. For trace metals there are two values: The top value is unfiltered samples. The lower value is filtered (0.45 µm) samples. See Appendix A for full list of trace metals that are included in one or more guideline.*

Parameter	Unit	L-06	L-06	L-07	L-07	L-08	L-08	Guideline limit
Date of sampling	Date	June 2018	Sep. 2018	June 2019	Sep. 2018	June 2019	Sep. 2019	-
pH_{field}	-	7.04	6.78	6.9	6.81	6.26	6.56	6.5-8.0
$Conductivity_{field}$	mS/m	2.83	1.23	0.82	0.88	1.19	0.76	<250
$Temp_{field}$	°C	5	6.3	5.7	4.3	6.7	7.4	-
$Alkalinity_{lab}$	meqv/l	0.10	0.08	0.07	0.07	0.039	0.04	-
F^-	mg/L	0.08	0.05	<0.04	<0.04	<0.04	<0.04	1.5
Cl^-	mg/L	3.60	0.64	0.18	0.15	1.47	0.48	250
NO_3^-	mg/L	0.09	<0.05	0.07	0.06	<0.05	<0.05	44
PO_4^{3-}	mg/L	<0.05	<0.05	<0.05	<0.05	<0.05	<0.05	-
SO_4^{2-}	mg/L	1.62	0.67	0.41	0.43	1.08	0.78	250
Na^+	mg/L	1.87	0.57	0.25	0.23	0.91	0.49	175
K^+	mg/L	0.51	0.30	0.41	0.38	0.24	0.21	-
Ca^{2+}	mg/L	2.32	1.37	0.89	0.98	0.78	0.66	-
Mg^{2+}	mg/L	0.43	0.19	0.12	0.11	0.21	0.16	50
Aluminum (Al)	µg/L	1100 15	560 17	1000 3.4	1100 5.1	81 4.3	900 8.8	200
Antimony (Sb)	µg/L	< 0.2 < 0.2	< 0.2 < 0.2	< 0.2 < 0.2	< 0.2 < 0.2	< 0.2 < 0.2	< 0.2 < 0.2	5
Arsenic (As)	µg/L	0.093 < 0.03	0.046 < 0.03	< 0.03 < 0.03	< 0.03 < 0.03	< 0.03 < 0.03	< 0.03 < 0.03	5
Barium (Ba)	µg/L	22 7.5	14 4.2	15 1.5	16 1.3	1.5 < 1	11 < 1	700
Lead (Pb)	µg/L	0.68 < 0.025	0.57 < 0.025	0.24 < 0.025	0.26 < 0.025	< 0.025 < 0.025	0.26 0.038	10
Boron (B)	µg/L	3.4 5.3	1.4 1.3	< 1 < 1	2.5 2.2	< 1 < 1	< 1 < 1	300
Cadmium (Cd)	µg/L	0.0088 < 0.003	< 0.003 < 0.003	< 0.003 < 0.003	0.0048 < 0.003	< 0.003 < 0.003	< 0.003 0.0035	3
Chromium (Cr)	µg/L	2.2 0.069	0.48 < 0.03	0.81 < 0.03	1.3 < 0.03	< 0.03 < 0.03	2.6 0.1	50
Cobalt (Co)	µg/L	0.72 < 0.04	0.38 < 0.04	0.54 < 0.04	0.63 < 0.04	0.07 < 0.04	0.99 < 0.04	5
Copper (Cu)	µg/L	1.7 0.37	1.6 0.26	1.9 < 0.03	9.8 0.13	< 0.03 < 0.03	3.3 0.62	1000
Nickel (Ni)	µg/L	1.3 0.049	0.52 0.066	1.1 < 0.03	1.4 < 0.03	0.40 0.067	3.9 0.24	20
Selenium (Se)	µg/L	0.058 < 0.05	< 0.05 < 0.05	< 0.05 < 0.05	< 0.05 < 0.05	< 0.05 < 0.05	< 0.05 0.061	10
Zink (Zn)	µg/L	3.6 0.4	1.9 < 0.3	3.6 4.2	6.5 < 0.3	0.44 0.55	4.6 1	100

Table 9 (Continued)

Parameter	Unit	L-09	L-09	L-10	L-10	Guideline limit
Date of sampling	Date	June 2019	Sep. 2019	June 2019	Sep. 2019	-
pH_{field}	-	6.6	6.58	6.95	7.34	6.5-8.0
$Conductivity_{field}$	µS/cm	1.0	0.65	1.05	3.07	<250
$Temp_{field}$	°C	5.2	6.8	5.6	1.6	-
$Alkalinity_{lab}$	meqv/l	0.035	0.03	0.067	0.22	-
F^-	mg/L	<0.04	<0.04	<0.04	<0.04	1.5
Cl^-	mg/L	1.41	0.46	0.23	0.27	250
NO_3^-	mg/L	0.079	<0.05	<0.05	0.08	44
PO_4^{3-}	mg/L	<0.05	<0.05	<0.05	<0.05	-
SO_4^{2-}	mg/L	1.08	0.78	0.76	3.88	250
Na^+	mg/L	0.75	0.35	0.25	0.06	175
K^+	mg/L	0.11	0.08	0.45	0.22	-
Ca^{2+}	mg/L	0.71	0.61	1.10	0.32	-
Mg^{2+}	mg/L	0.22	0.11	0.24	0.11	50
Aluminum (Al)	µg/L	9.7 3.0	22 3.8	1000 2.8	140 4.9	200
Antimony (Sb)	µg/L	< 0.2 < 0.2	< 0.2 < 0.2	< 0.2 < 0.2	< 0.2 < 0.2	5
Arsenic (As)	µg/L	< 0.03 < 0.03	< 0.03 < 0.03	< 0.03 < 0.03	< 0.03 0.036	5
Barium (Ba)	µg/L	< 1 < 1	< 1 < 1	39 3.8	14 9.6	700
Lead (Pb)	µg/L	0.14 0.11	0.029 < 0.025	0.14 < 0.025	0.03 < 0.025	10
Boron (B)	µg/L	< 1 < 1	< 1 < 1	< 1 < 1	< 1 < 1	300
Cadmium (Cd)	µg/L	< 0.003 < 0.003	< 0.003 < 0.003	< 0.003 < 0.003	< 0.003 < 0.003	3
Chromium (Cr)	µg/L	< 0.03 < 0.03	< 0.03 0.05	4.8 < 0.03	0.73 0.17	50
Cobalt (Co)	µg/L	0.16 0.10	< 0.04 < 0.04	1.2 < 0.04	0.18 < 0.04	5
Copper (Cu)	µg/L	< 0.03 < 0.03	0.24 0.24	2.9 < 0.03	0.67 0.19	1000
Nickel (Ni)	µg/L	0.20 0.062	0.07 0.15	8.3 0.1	21 0.47	20
Selenium (Se)	µg/L	< 0.05 < 0.05	< 0.05 < 0.05	< 0.05 < 0.05	< 0.05 0.071	10
Zink (Zn)	µg/L	23 23	< 0.3 < 0.3	3.6 6.7	< 0.3 0.4	100

7.3 Radioisotopes

Radioactivity from natural mineral sources is unwanted in drinking water and is generally not expected to be an issue. Yet, radioactive minerals are present in parts of Greenland and it was therefore chosen to include analysis of the most common radioactivity parameters, which for the EU and Denmark is “total indicative dose” and “tritium” and for the International Council of Bottled Water Associations “’total alpha- and beta-activity”. It should be noted that the detection limits of radioactivity parameters provided by the commercial laboratory varies from day to day but for alpha- and beta-activity in general are close to the guideline limits, which makes it difficult to conclude on samples containing small amounts of radioactivity close to the guideline limit. However, none of the investigated samples were anywhere near the guideline limits. In fact, only one sample exhibited a detectable level of alpha-activity and this was well below the guideline limit. All data are seen in Table 10.

Table 10. *Radioactivity parameters.*

Parameter	Unit	L-06	L-06	L-07	L-07	L-08	L-08	L-09	L-09	L-10	L-10	Guideline limit*
Date of sampling	Date	June 2018	Sep. 2018	June 2019	Sep. 2018	June 2019	Sep. 2019	June 2019	Sep. 2019	June 2019	Sep. 2019	-
Total indicative dose	mSv/yr	< 0.1	< 0.1	< 0.1	< 0.1	< 0.1	< 0.1	< 0.1	< 0.1	< 0.1	< 0.1	0.1
Total alpha-activity	Bq/L	<0.027	< 0.13	< 0.04	0.012	< 0.04	< 0.05	< 0.04	< 0.04	< 0.04	< 0.05	0.1
Total beta-activity	Bq/L	< 0.19	<0.563	< 0.4	<0.183	< 0.4	< 0.4	< 0.4	< 0.4	< 0.4	< 0.4	1
Tritium activity	Bq/L	< 5	< 9	< 10	< 9	< 10	< 10	< 10	< 10	< 10	< 10	100

*Total indicative dosis and tritium as regulated in the EU and Denmark. Total alpha and beta activity as indicated in the International Council of Bottled Water Associations standards (ICBWA).

7.4 Sediment

Glacial meltwater always contain some suspended solids also known as sediment. The sediment is produced by erosion of the basal rock as the glacier moves over the terrain.

It is this sediment that makes the lakes and rivers in Greenland vary in colour, from clear and dark to blueish, ”milky”, grey and brown. The difference in colour is due to the variation in the content of sediment (rock in particle form), which is found in different concentrations (mg/L) in the water. Rivers may also differ quite substantially; in some valleys, rivers wind through green areas within a single riverbed whereas in other valleys, rivers form vast networks of braided channels taking up the entire vegetation-free valley floor. When investigating the origin of the braided river systems, they most often derive from local glaciers or the inland ice. The erosion of the glacier ice of the basal material produces the sediment as the glacier moves over the terrain. This form of erosion is one of the most powerful on the Earth. Water originating from melting local glaciers or the Greenland Ice Sheet will thus always contain a certain amount of sediment.

The largest concentrations of sediments are observed where the meltwater leaves the glacier. The concentration of sediment decreases downstream as stream-power generally decreases. Moreover, the presence of proglacial lakes between the ice and the outlet location act as natural sediment traps that filter away the coarser sediments and thus reduces the sediment concentration. Once the sediment-laden water reaches the fjord, it will appear as

plumes in front of the river mouths. The resulting sediment concentration has an influence on the required filtering treatment following extraction of water. An example of water flow through proglacial lakes and sediment plumes in the fjord is illustrated in Figure 27.

Figure 27. *Example of water flow, a sediment plume, and proglacial lakes in a catchment. As water flows through the proglacial lakes, these as act as natural sediment traps filtering away sediments. Once the water reaches the fjord the outflow of water containing the remaining sediment will appear as a plume in the surface layers of the fjord water. The base-map is a summer 2018 optical Sentinel-2 satellite image.*

There is no guideline limit for sediment content in drinking water, but there is a guideline limit for turbidity of 1 NTU (nephelometric turbidity units) in potable water, corresponding roughly to 2 mg/L of suspended sediment (but the relationship between sediment content and turbidity may vary substantially depending on the sediment type and size).

The amount of sediment was determined from three (2018) or four (2019) 1L-samples, that were individually filtered through a 0.45 µm pre-weighed filter. The filter was then dried and weighed again to determine the sediment content in mg/L. A subsample of at least 30 mg dried sediment was then used to determine grain size distribution on a Malvern particle size analyzer. In cases where less than ~30 mg dried material was available, sediment from all replicates was pooled before analysis and thus only one analysis of size distribution is available. In cases with less than ~10 mg/L sediment size distribution could not be deter-

mined. The streams containing < 10 mg/L sediment were typically those with lakes between glacier and sampling point. Since large sediment particles settle more easily than finer grained particles, finer particles are more likely to be transported all the way to the sea if lakes exist along the stream pathway. The particles present at the outlet of these streams are therefore most likely very fine (a few tens of µm or smaller).

Table 11. *Average sediment concentration ± standard deviation (three or four 1L replicates).*

Parameter	Unit	L-06	L-07	L-08	L-09	L-10	Guideline*
Sediment, June	mg/L	13 (1.2)	23 (0.7)	1.3±0.5	0.5±0.1	163±7	-
Sediment, Sept.	mg/L	20 (0.7)	34 (0.3)	143±44	0.3±0.3	5.3±0.8	-

*There is no guideline limit for sediment content, but there is a guideline limit for turbidity of 1 NTU (nephelometric turbidity units), corresponding roughly to 2 mg/L of suspended sediment (but this may vary).

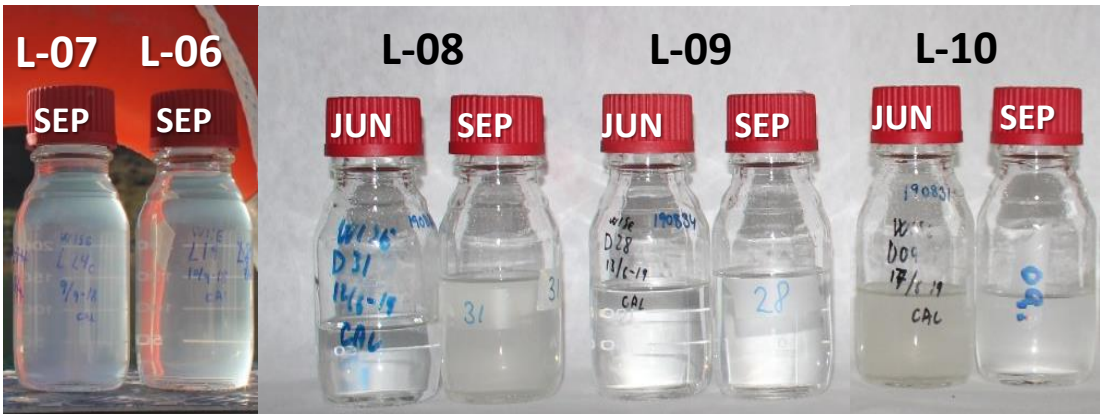

Figure 28. *Visible difference in sediment content of the water. From left to right: Sample from L-07 (34 mg/L, September 2018), L-06 (20 mg/L, September 2018), L-08 (1 and 143 mg/L, June and September 2019), L-09 (0.5 and 0.3 mg/L, June and September 2019) and L-10 (163 and 5 mg/L, June and September 2019).*

7.4.1 Grain size distributions for streams visited in 2018 and 2019

After filtration, sediment was scraped off the filters and analyzed for their grain size distribution. In Figure 29 the particles are divided into four size-fractions (clay-sized (<2 µm), fine silt (2-16 µm), coarse silt (16-63 µm) and sand (>63 µM) for each site. In Figure 30, the raw particle size distributions are shown.

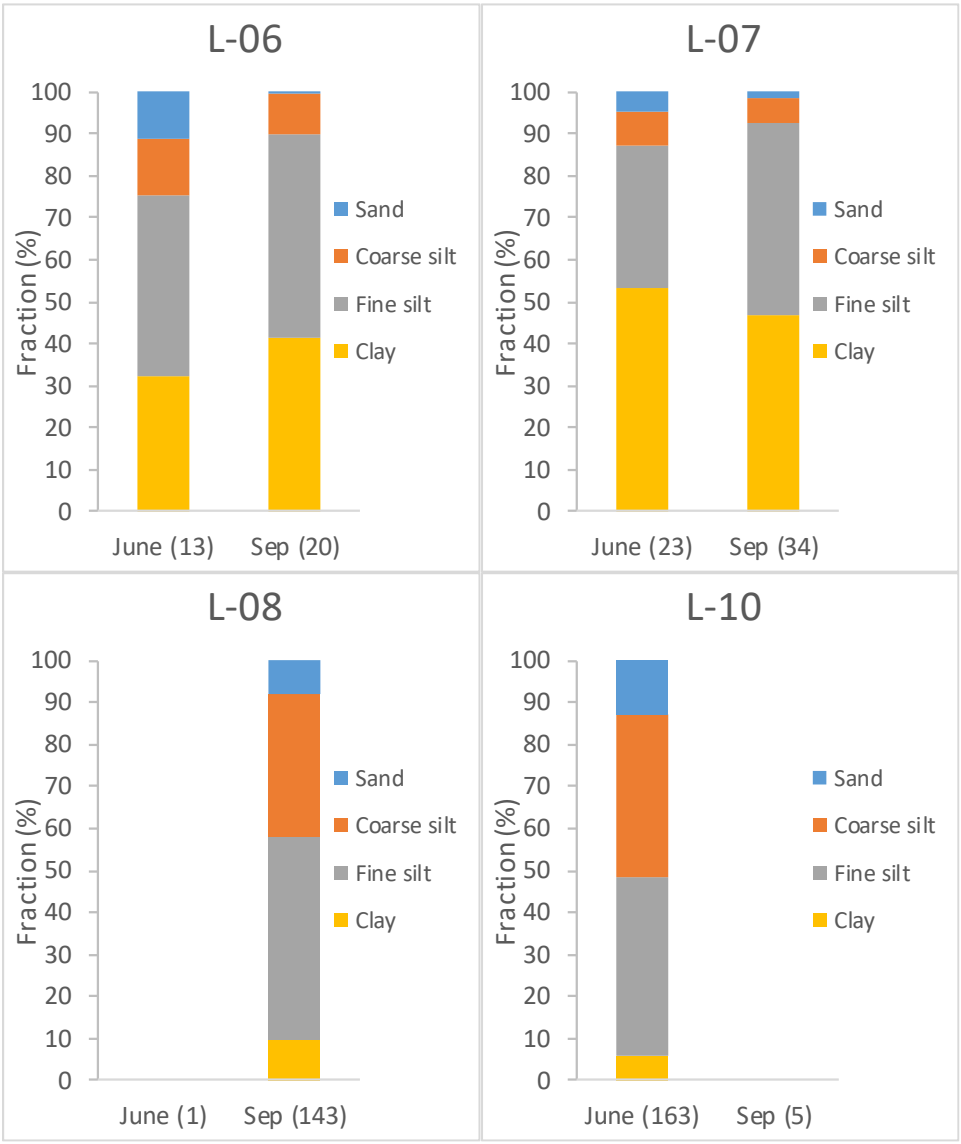

Figure 29. *Grain size distribution divided into four size fractions (clay-sized (<2 µm), fine silt (2-16 µm), coarse silt (16-63 µm) and sand (>63 µM)). Some streams contained too little sediment to perform grain size distribution. Site L-08 and L-10 contained enough sediment at only one of the visits. The amount of sediment in mg/L is indicated in parenthesis at the x-axis (see also Table 11).*

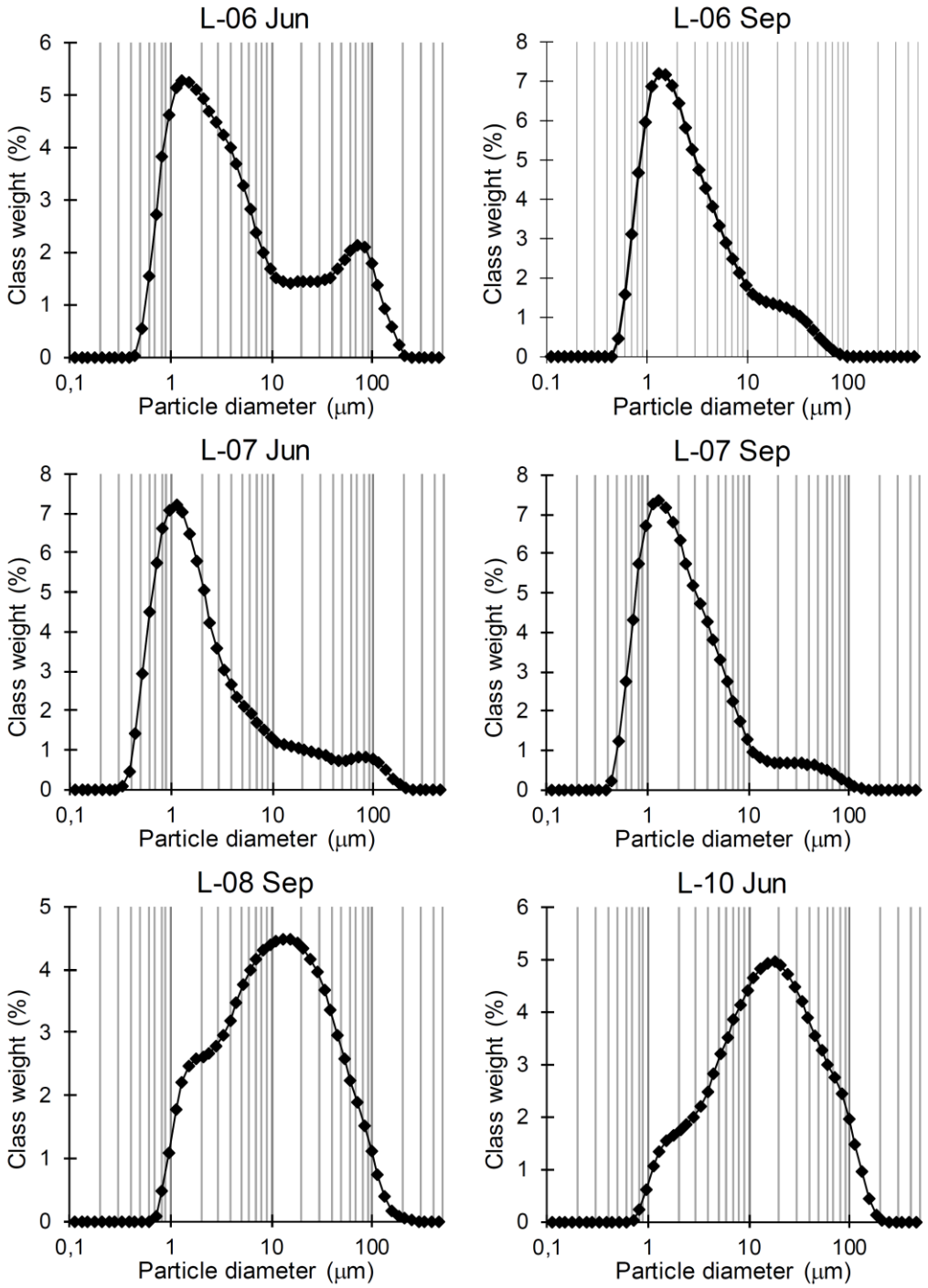

Figure 30. *Grain size distribution for all streams in June and September. Some streams contained too little sediment to perform grain size distribution. Site L-08 and L-10 contained enough sediment at only one of the visits.*

The amount as well as the distribution between coarse and fine sediment is important with regards to how the purification of the water should be done to fulfill the guideline limit of 1 NTU. Sand and coarse silt may settle quite fast while clay-sized particles and fine silt will probably need to be removed by some sort of filtration.

7.5 Water isotopes ($\delta^{18}O$ and $\delta^{2}H$)

Water contains the two elements: Oxygen (O) and hydrogen (H). Most of the oxygen is the isotope ^{16}O and most of the hydrogen is the isotope ^{1}H. However, a small fraction of the water molecules contains one of the heavier isotopes ^{18}O and ^{2}H containing two or one neutrons more than their respective dominating isotopes. In precipitation, there is a fractionation of isotopes, so that the colder it is when the precipitation is formed, the lower the amount of heavy isotopes. This means that ice from the Greenlandic Inland Ice will have a lighter signature (more negative $\delta^{18}O$-value) than snow falling at the coast during winter, which again will have a lighter signature than rain falling in the summertime. This pattern is also seen in the precipitation and ice samples we collected in 2018 and 2019 (Table 12 and Table 13).

Table 12. *$\delta^{18}O$ values in rain, snow and Inland Ice collected in June and September 2018 with an average containing a larger number of samples from similar locations. Snow in June was from patches probably containing a mixture of snow from different time points in winter and with refrozen spring rain mixed in. A sample from L-08 in 2019 is also shown.*

	L-06 June	Narsaq beach	Avg. 2018	L-08 Sep
Rain			-14.4	-13.3
Snow	-16.8		-15.7	
Ice		-24.7	-22.4	

Table 13. *$\delta^{2}H$ values in rain, snow and Inland Ice collected in June and September 2018 with an average containing a larger number of samples from similar locations. Snow in June was from patches probably containing a mixture of snow from different time points in winter and with refrozen spring rain mixed in. A sample from L-08 in 2019 is also shown.*

	L-06 June	Narsaq beach	Avg. 2018	L-08 Sep
Rain			-108.6	-89.9
Snow	-123.7		-119.8	
Ice		-185.8	-168.0	

By comparing the isotope signatures in precipitation, Inland Ice, local glacial ice and the streams, one may calculate a rough estimate of the fraction of glacial meltwater in the stream (Table 14 and Table 15). The streams visited in 2018 (including L-06 and L-07) are all outlets from the Inland Ice. The streams visited in 2019 are, on the other hand, all outlets from local glaciers (including L-08 and L-09) or a local ice cap (L-10). Local glaciers and ice caps may have very different isotope signatures compared to the Inland Ice due to different altitudes of the ice-forming areas. Preferably, one should have ice samples from each local glacier to make a proper calculation of the fraction of melted ice. We had good measurements of the local ice cap feeding L-10. However, for L-08 and L-09 we have no good

measurements of ice samples and we therefore cannot estimate the fraction of melted ice at these locations.

For the June 2018 samples, we used average values for the 2018 snow samples as precipitation for this calculation. For the September 2018 samples, we used a rain sample as precipitation. For the June 2019 samples, we used values for a snow sample taken near L-10 as precipitation for this calculation. For the September 2019 samples, we used the rain sample taken at L-08 on September 6th as precipitation.

Table 14. *$\delta^{18}O$ values and rough calculations of % input from glacial meltwater in June and September. The wide range of values ranging from below zero to above 100 % reflects the very rough nature of the estimation method.*

ID	June	Sep	% ice June	% ice Sep
L-06	-14.8	-16.1	-15	22
L-07	-18.9	-18.7	48	55
L-08	-16.7	-16.0		
L-09	-17.7	-16.6		
L-10	-20.5	-19.1	101	82

Table 15. *$\delta^{2}H$ values and rough calculations of % input from glacial meltwater in June and September.*

ID	June	Sep	% ice June	% ice Sep
L-06	-107.6	-118.1	-24	16
L-07	-138.7	-137.9	40	49
L-08	-118.5	-114.4		
L-09	-127.3	-121.3		
L-10	-152.1	-141.1	109	86

L-06 contains little Inland Ice and L-07 contain some Inland Ice, especially in September. L-10 was mainly glacial meltwater in both June and September. No safe conclusions can be made for L-08 and L-09 due to the lack of ice samples, but their isotope signatures do all point to some ice contribution and probably a higher fraction of meltwater in L-09 than in L-08 in both June and September.

It should be stressed that the fractions of glacial meltwater calculated in Table 14 and Table 15 are *very* rough estimates. The presence of lakes upstream will also influence the isotope signature if the residence time in the lake is long enough for significant evaporation to occur. In such a case, the isotope values of the downstream stream will be even heavier (less negative) and the content of Inland Ice may appear negative. The heavy isotope signature of L-06 in June is thus probably a result mainly of very low input from Inland Ice and precipitation with relatively heavy isotope signature in the area. Despite these uncertainties, the main conclusions on which streams have a significant contribution of Inland Ice and which do not, should be reasonable. Especially so, since it in general fits with the sediment data (more sediment in those streams that indicate a more significant contribution from Inland Ice), see the section on sediment content. Also for L-10, it seems reasonable to conclude that most water is meltwater from the the local ice cap.

7.6 Microbiology

7.6.1 Bacterial counts (CFU)

When water is bottled, it should as a minimum fulfil the Danish microbiological criteria described in the guideline "*Bekendtgørelse om naturligt mineralvand, kildevand og emballeret drikkevand*" (BEK nr 38 af 12/01/2016).

Table 16. *Danish microbiological guideline limits for bottled water (BEK nr 38 af 12/01/2016).*

Parameter	Guideline limit
Escherichia coli (37°C and 44.5°C)	0/250 ml
Coliform bacteria (37°C and 44.5°C)	0/250 ml
Enterococcus faecalis	0/250 ml
Sporulating sulfite-reducing anerobic bacteria	0/50ml
Pseudomonas aeruginosa	0/250 ml
Parasites and pathogenic microorganisms	Not detected
CFU* at 20-22°C	100/ml
CFU* at 37°C	20/ml

*Colony forming units

For coli bacteria, the guideline actually says: "No *Escherichia coli* or other coli bacteria in 250 mL at 37°C and 44.5°C". We interpret "other coli bacteria" as no coliform bacteria. The microbial analyses should be carried out by an accredited laboratory. For drinking water, CFU counts should generally be initiated by the laboratory within 24 hours after sampling or within 12 hours after bottling, which is not possible with the logistical challenges during fieldwork conducted over large distances in Southwest Greenland. We have therefore made a simpler screening at field condition using the Petrifilm method. Results from this method are not as precise as when the samples are analyzed by an accredited laboratory in nutrient agar. We have used petrifilm to analyze total CFU (3M petrifilm Aqua 6450/6452 heterotrophic incubated at 22°C), thermotolerant CFU (3M petrifilm Aqua 6450/6452 heterotrophic at incubated at 36°C), coliform bacteria (3M petrifilm Aqua 6457/6458 coliform) and bacteria from the group *Enterobacteriaceae* (3M petrifilm Aqua 6418/6428 *Enterobacteriaceae*).

Coliform bacteria is a group of bacteria, of which many are intestinal. Since *E. coli* is a subgroup of the coliform bacteria, this means that if no coliform bacteria are present, there are also no *E. coli* in the samples. *Enterobacteriaceae* is a large family of gram-negative bacteria, of which many are intestinal. The presence of coliform and/or *Enterobacteriaceae* are therefore indicators of fecal contamination though both may be present in low densities in many non-polluted environments. The counts for fecal indicator species performed on-site are not exactly as those demanded in the microbiological guideline for bottled water (BEK nr 38 af 12/01/2016), but they are judged sufficient for a screening phase.

The petrifilms for total CFU were, as far as possible incubated as described in DS/EN ISO 6222 (Enumeration of culturable microorganisms in a nutrient agar at 22°C and 36°C), with

the deviation that CFU were determined using petrifilm instead of seeding in yeast extract agar. The ISO standard notes that CFU should be incubated at 22 ±2°C for 68 h and at 36 ±2°C for 44±4 h, so there is a deviation between the ISO-standard and the Danish guideline.

Petrifilm for counting coliform bacteria and *Enterobacteriaceae* were incubated at 36±2°C for 21±3 hours, as described in DS/EN ISO 9308-1 (water quality – Enumeration of *Escherichia coli* and coliform, part 1). This guideline also deviates slightly from the Danish Guideline. After incubation, the films were stored at approximately 5°C and counted within 12 hours. On 3M coliform petrifilm, true coliforms produce acid (faint pink halo associated with colonies) and are associated with gas bubbles. In the field, it was hard to determine the presence of bubbles and haloes, we therefore counted all colonies as coliforms. This validity of this assumption was demonstrated for selected samples by growth on MacConkey agar at 37°C and by DNA sequencing (see below).

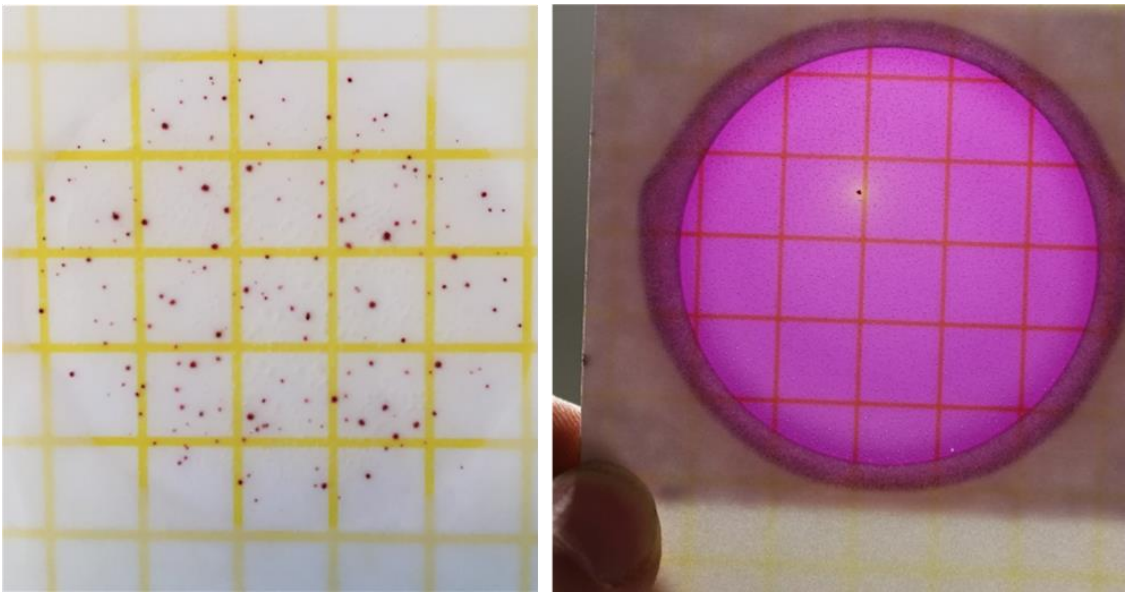

Figure 31. *Examples of petrifilm results for total CFU at 22°C (left) and Enterobacteriaceae (right, one CFU).*

The petrifilms were incubated in custom-made, mobile incubators, since the power source available was 12V lead-acid batteries. The temperature in each incubator was monitored with a datalogger. The temperature in the 22°C-incubator varied from 20 to 24°C during incubation, which is also within the prescription of the ISO-standard (22 ±2°C). The 36°C-incubator generally varied from 34 to 38°C, which is within the prescription of the ISO-standard, but the temperature was lower for some samples during the 2019 September campaign (Table 17). The effects of reduced temperature was investigated and found to be of minor importance for coliform and *Enterobacteriaceae* counts (see below), whereas counts of total thermotolerant CFU were discarded for samples from the September 2019 campaign.

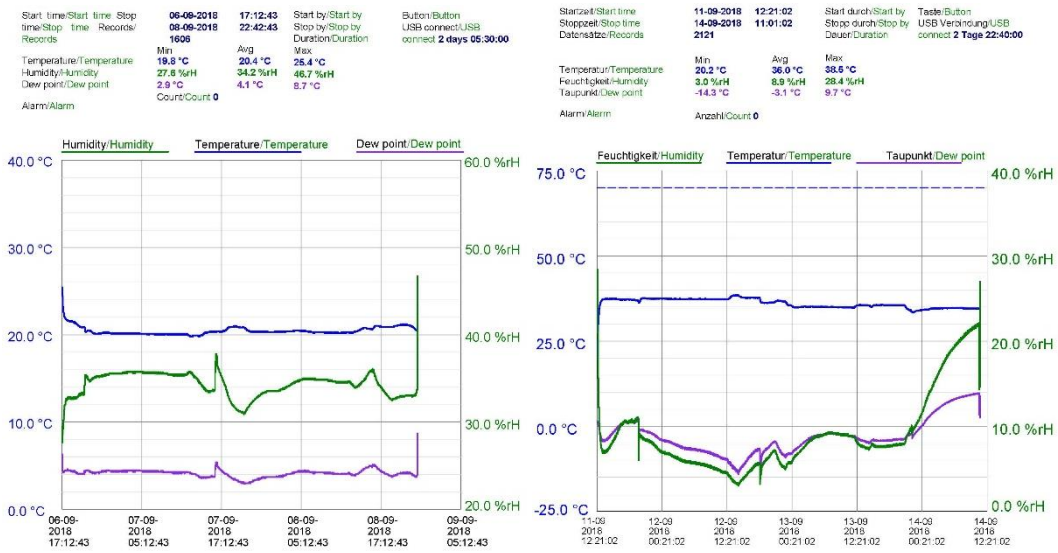

Figure 32. *Examples of typical temperature fluctuations in 22°C (left) and 36°C (right) incubators. The blue line is temperature.*

The results of the bacterial counts are presented in Table 17. CFU counts at 22°C was close to the guideline limit or exceeded the limit for several streams. There were no systematic differences between the June and September counts. CFU at 36°C, on the other hand was below the guideline limit. Coliform bacteria were detected (i.e. exceeded the guideline limit) in most streams. L-09 and had high counts of 13 coliforms mL^{-1} in the September campaign. The *Enterobacteriaceae* petrifilms generally showed counts similar to the coliform petrifilms.

Table 17. *Bacterial counts (CFU) per mL water in the streams. Numbers were calculated from five counts of 1 mL, except Total CFU, which was calculated from five counts of 1 mL and five counts of 0.1 mL (10x dilutions).*

ID	Sampling time	CFU at 22°C, mL^{-1}	CFU at 36°C, mL^{-1}	Coliform bacteria, mL^{-1}	*Enterobacteriaceae*, mL^{-1}
L-06	June, 2018	105	5.6	0.2	0.6
L-06	September, 2018	92	11	4.4	2.4
L-07	June, 2019	65	1.8	0.2	<0.2
L-07	September, 2018	41	4	0.8	0.4
L-08	June, 2019	44	11.4	1.6	1.8
L-08	September, 2019	232	- [a]	1.8 [b]	1.4 [b]
L-09	June, 2019	50	2.4	0.6	0.4
L-09	September, 2019	159	- [a]	13 [b]	3.6 [b]
L-10	June, 2019	38	0.4	<0.2	<0.2
L-10	September, 2019	110	- [a]	0.5 [b]	0.7 [b]
Guideline limit		≤100	≤20	<0.004*	-

*0 in 250 mL

[a] No data, petrifilm incubated at too low temperature.

[b] Incubated at 20-34°C

[c] Extended storage, water sample stored at 2-5°C for 49 hours before inoculation of petrifilms.

To summarize the microbiological assessment, we recommend gentle water treatment (e.g. UV-irradiation) at all locations as is common for surface water.

For all streams assessed to be suitable for exploitation, we recommend testing for all microbiological parameters prescribed in the guideline (Table 16) and to repeat the analyses throughout a season. The microbiological parameters should be determined by an accredited laboratory. If a site is chosen for production, we furthermore recommend testing repeatedly for enteric parasites (*Cryptosporidium*).

7.6.2 Further characterization of colonies on coliform- and *Enterobacteriaceae* petrifilms

We sequenced the 16s rRNA gene from 96 randomly selected colonies from the *Enterobacteriaceae*- or coliform petrifilms from the 2019 campaign to gain more information on which types of bacteria, that were detected by the coliform and *Enterobacteriaceae* counts. This also included testing of growth at 37°C, which was especially important for the petrifilms from the September campaign as these were accidentally incubated at reduced temperature, i.e. this was also a test for false positives. The coliform colonies were also tested for growth at 44.5°C to test for the presence of thermotolerant (faecal) coliforms.

The coliform- and *Enterobacteriaceae* petrifilms were stored cold during transport to Copenhagen. Ninety-nine randomly selected colonies from the petrifilms were streaked on MacConkey agar plates followed by incubation at 37°C. MacConkey agar is a selective and differential culture medium commonly used for the isolation of enteric gram-negative bacteria. DNA was extracted from the MacConkey agar colonies, and the colonies identified by partial sequencing of their 16S rRNA gene.

Forty-five colonies from coliform petrifilms all grew on MacConkey agar when incubated at 37°C. None of them, hovever, grew on MacConkey agar at 44.5 °C, in other words, none of them were thermotolerant faecal coliforms. All colonies belonged to the family *Enterobacterioaceae* within the order *Enterobacteriales* (Table 18). The most common genus was *Rahnella* that constituted 45% of the original colonies. According to Rozhon et al. (2010), *Rahnella* is a genus ”commonly found in the rhizosphere and phyllosphere, seeds, fruits, water and intestinal tracts of herbivores including snails, slugs, and even American mastodon remains.” There are reports of the species *Rahnella aquatilis* as a rare opportunistic pathogen mostly of immunocompromized patients (e.g. Tash, 2005; Harrel et al., 1989; Chang et al., 1999; and Kuzdan 2015). As we identified the colonies only to the genus level, it is unknown whether any of them actually belong to the species *Rahnella aquatilis.* The second and third most frequently isolated genera from the coliform petrifilms were *Yersinia* (31%) and *Serratia* (20%). *Yersinia* is common in the environment, but some strains are also well recognised pathogens of humans. *Serratia* are widespread in the environment but are not a common component of the human fecal flora (Donnenberg, 2010). The opportunistic pathogen *S. marcescens* occurs naturally in soil but is also associated with human infections.

Fifty-four colonies from *Enterobacteriaceae* petrifilms were streaked on MacConkey agar and 51 of them were viable at 37°C. Overall, only 3 out of the 99 tested colonies did not grow on the MacConkey agar. This shows that almost all counts on coliform- and *Enterobacteriaceae* petrifilms were able to grow at 37 °C, though some were enumerated at lower temperature. The sequence data from the *Enterobacteriaceae* petrifilms were in line with the results from the coliform petrifilms, though the *Enterobacteriaceae* petrifilms seem to be a little less specific with 6% of the isolates not belonging to the family *Enterobacteriaceae*. The similarity corresponds well with the similar CFU counts using these two types of petrifilm (Table 17). The most common genus from the *Enterobacteriaceae* petrifilms was again *Rahnella*, followed by *Serratia* (22%) and *Yersinia* (12%).

Interestingly, none of the sequenced colonies were *E. coli*, which is in line with the absence of growth at 44.5 °C. It should therefore be stressed that the sequenced isolates, and thus the coliform counts, are environmental strains and not indicators of fecal contamination.

Table 18. *Identification (taxonomic affiliation) of 16S rRNA gene sequences from colonies counted on either coliform or Enterobacteriaceae petrifilms from the 2019 field campaign. Numbers of sequenced colonies are also reported as percentage of the total number of sequenced colonies for each petrifilm type.*

Petrifilm	Number of colonies	Order	Family	Genus
Coliform	1 (2%)	*Enterobacteriales*	*Enterobacteriaceae*	*Ewingella*
	1 (2%)	*Enterobacteriales*	*Enterobacteriaceae*	*Moellerella*
	2 (4%)	*Enterobacteriales*	*Enterobacteriaceae*	*Obesumbacterium*
	18 (40%)	*Enterobacteriales*	*Enterobacteriaceae*	*Rahnella*
	9 (20%)	*Enterobacteriales*	*Enterobacteriaceae*	*Serratia*
	14 (31%)	*Enterobacteriales*	*Enterobacteriaceae*	*Yersinia*
Enterobacteriaceae	2 (4%)	*Enterobacteriales*	*Enterobacteriaceae*	*Ewingella*
	1 (2%)	*Enterobacteriales*	*Enterobacteriaceae*	*Hafnia*
	23 (45%)	*Enterobacteriales*	*Enterobacteriaceae*	*Rahnella*
	11 (22%)	*Enterobacteriales*	*Enterobacteriaceae*	*Serratia*
	6 (12%)	*Enterobacteriales*	*Enterobacteriaceae*	*Yersinia*
	5 (10%)	*Enterobacteriales*	*Enterobacteriaceae*	*Unidentified*
	1 (2%)	*Pseudomonadales*	*Moraxellaceae*	*Acinetobacter*
	1 (2%)	*Pseudomonadales*	*Moraxellaceae*	Unidentified
	1 (2%)	*Aeromonadales*	Unidentified	Unidentified

7.7 Cyanotoxins

Cyanobacteria are often the dominating, photosynthesizing bacteria in aquatic freshwater ecosystems in the Arctic (Calieri m.fl., 2012; Vincent m.fl., 2012). Cyanobacteria may occasionally produce large amounts of toxins of which microcystins (also known as cyanoginosins) are the most well-studied group (WHO, 2011). In contrast to many other cyanotoxins, microcystins are often cell-bound compounds, which may to some extent be removed from the water by sedimentation processes (WHO, 2011). A research paper from 2016 reported the presence of microcystins in 18 out of 18 lakes in Western Greenland (Trout-Haney et al., 2016). The levels varied from 0.005 to 0.4 µg/L. Based on those findings, the samples were analyzed for microcystins by a commercial lab. Another cyanotoxin, nodularin, was also included in the analyses. Cyanotoxins were not detected in any of the samples (Table 19). This result does not completely rule out the presence of cyanotoxins, since the detection limit at the commercial lab was 0.5-2.0 µg/L, which is higher than all findings in Trout-Haney et al. (2016). The analytical method used by Trout-Haney et al. (2016) was an immunochemical method (ELISA), with a very low detection limit. However, it does not discriminate between different microcystins and also gives a signal for nodularin, which has a similar chemical structure. Since earlier data were based on a different analytical principle, the results from Trout-Haney et al. (2016) are not directly comparable with our results in Table 19.

Microcystin LR is the most widespread cyanotoxin and the only cyanotoxin, with sufficient data for a threshold limit (WHO, 2011). The provisional guideline limit for microcystin LR (free + cell-bound) in drinking water is 1 µg/L (WHO, 2011). This value was not exceeded at any of the localities, but other microcystins may be present without detectable levels of microcystin LR. Cyanotoxins were not analyzed in later field campaigns, due to the high cost and the fact that microcystins were not detected in any of the tested samples in 2017 (Ahlstrøm et al., 2018) or 2018 (this report). Microcystins may, however, show seasonal variation, and we therefore recommend to monitor cyanotoxins throughout an entire season at potential production localities with upstream lakes.

Table 19. *Cyanotoxin analyses, September 2018.*

Parameter	Unit	L-06	L-07
Microcystin LW	µg/L	< 2	< 2
Microcystin LR	µg/L	< 0.5	< 0.5
Microcystin RR	µg/L	< 0.5	< 0.5
Microcystin YR	µg/L	< 0.5	< 0.5
Nodularin	µg/L	< 0.5	< 0.5

8. Conclusion

This report contains information on five selected locations that may be utilized for industrial collection of drinking water. This report is not aimed at addressing any technical or engineering questions posed by the locations or water treatment, but only concerns the natural environment and the quality of the water as it was sampled. A prerequisite in the investigation has been that the water should be at least partly derived from meltwater originating either from the Greenland Ice Sheet or from local glaciers and ice caps.

The selection of locations described in Ahlstrøm et al. (2018) and updated in Kjeldsen et al. (2019), was based on a three-level approach: accessibility, abundance and water quality, where each level is dependent on the former. At each level, a number of different criteria was identified and assigned a weight in the assessment with the goal to single out the most promising locations to visit in the field. The accessibility criteria included proximity to infrastructure, marine chart coverage, availability of bathymetry data, river slope, and abundance of sea ice and icebergs, respectively. The abundance criteria related to water discharge, length of the melt season, existence of proglacial lakes, risk of outburst floods, upstream catchment changes, total ice cover within the catchment and ice cover relative to catchment size. Finally, the water quality criteria focused on origin of the water, age of the source ice, expected sediment concentration in the meltwater and other issues from contact with naturally occurring minerals.

Locations are defined as outlets of a significant meltwater river to accessible fjords in the southwestern part of Greenland, to minimize potential sea ice and iceberg interference. Catchments for each location or river outlet were derived employing advanced hydrological methods, using the most recent elevation models available.

Subsequently, results from a regional climate model were used as input to a glacio-hydrological model to calculate the average monthly discharge expected at each location from precipitation and meltwater leaving the catchment. The five locations represent very different catchment sizes with varying amounts of discharge, ranging from roughly 290,000 million litres per year for L-07, down to slightly over 10,000 million litres per year for L-09. The rivers at all locations are, on average, discharging water from May to November with the vast majority of water discharging in the period June-September.

A comparison between modelled discharge for the catchments for the two periods 1980-1991 and 2006-2017, showed an increase in the discharge at all sites except L-06, which was stable at slightly over 21,000 million litres per year. A similar method was also used to examine the change in discharge over the last few decades, showing a promising overall melt increase of more than 50 % for the region.

The five selected locations were visited by boat to sample the water and collect additional data. The field visits were conducted in June and September in either 2018 or 2019, to capture the seasonal variability in the water quality. Two locations, L-06 and L-07, drain ice sheet catchments and three locations, L-08, L-09 and L-10, drain catchments with local mountain glaciers and ice caps.

An extensive analysis of chemical, physical and microbiological parameters was performed on the water samples. Some types of analyses had to be performed on-site, some were performed at GEUS laboratories and some at certified commercial laboratories.

All of the locations provide large amounts of meltwater during the summer from June-September, with river outlets relatively near deep fjord waters. The meltwater contains varying amounts of sediment derived from glacier erosion of the bedrock, requiring filtration of the meltwater before use. For all five locations, inorganic parameters are below drinking water requirements and guidelines in filtered water samples. Gentle UV-treatment is recommended for the water from all locations, as is commonly required for surface-derived water, as microbiological parameters are generally exceeding the guideline limits.

For convenience, we have summarized the findings from each of the five locations separately below:

L-06

Total catchment area of 20.2 km^2, including 2.3 km^2 of ice sheet area, with ice of Holocene origin. Estimated mean discharge of 21,400 million litres per year, with the vast majority discharging from June to September. No apparent risk of outburst floods. L-06 contained some sediment in both June and September (13-20 mg/L) of which a bit is coarse sediment, especially in June, but most of the sediment consisted of fine silt and clay-sized particles.

L-06 exceeded guideline limits for aluminum in unfiltered samples, but when sediment was removed, values were well below limits. L-06 showed no sign of radioisotopes. L-06 contained some sediment in both June and September (13-20 mg/L) of which a bit is coarse sediment, especially in June, but most of the sediment consisted of fine silt and clay-sized particles. All meltwater at L-06 runs through four minor lakes, which seem to remove most coarse sediment. With regards to microbiological parameters, CFU at 22°C was close to the guideline limit in both June and September, with a small exceedance in June. CFU at 36°C were well below the guideline limit. Coliform bacteria were detected, i.e. exceeded the guideline limit in both June and September.

L-07

Total catchment area of 279.5 km^2, including 91.5 km^2 of ice sheet area and 8.8 km^2 of local ice cap area, with ice of Holocene and late Holocene origin. Estimated mean discharge of 291,100 million litres per year, with the vast majority discharging from June to September. Minor lake at ice margin, but low apparent risk of outburst floods. L-07 contained some sediment in both June and September (23-34 mg/L). The sediment was mainly clay-sized and fine silt.

L-07 exceeded guideline limits for aluminum in unfiltered samples, but when sediment was removed, values were well below the limit. L-07 showed no sign of radioisotopes except for a very small alpha-activity in September. L-07 contained some sediment in both June and September (23-34 mg/L) and the sediment was mainly clay-sized and fine silt, probably because all meltwater runs through a major lake. With regards to microbiological parameters, CFU at 22°C and 36°C were below the guideline limit in both June and September, but coliform bacteria were detected, i.e. exceeded the guideline limit.

L-08

Total catchment area of 50.0 km^2, including 18.6 km^2 of local ice cap area, with ice of late Holocene origin. Estimated mean discharge of 73,500 million litres per year, with the vast majority discharging from June to September. No apparent risk of outburst floods. L-08 contained very little sediment in June (1.3 mg/L) but significant amounts in September (143 mg/L). In September, the sediment consisted mainly of fine and coarse silt, but also with a significant fraction of both clay-sized particles and sand.

L-08 exceeded guideline limits for aluminum in unfiltered samples in September, but when sediment was removed, the value was well below the limit. The stream showed no sign of radioisotopes. L-08 contained very little sediment in June (1.3 mg/L) but significant amounts in September (143 mg/L). In September, the sediment consisted mainly of fine and coarse silt, but also with a significant fraction of both clay-sized particles and sand, which probably reflects that most of the meltwater runs through some major lakes but a small fraction does not run through lakes. With regards to microbiological parameters, CFU at 22°C exceeded the guideline limit in September, and coliform bacteria were detected, i.e. exceeded the guideline limit, in both June and September.

L-09

Total catchment area of 9.4 km^2, including 5.0 km^2 of local ice cap area, with ice of late Holocene origin. Estimated mean discharge of 10,500 million litres per year, with the vast majority discharging from June to September. No apparent risk of outburst floods. L-09 contained almost no sediment in both June and September (0.3-0.5 mg/L).

L-09 contained very little trace metals even in unfiltered samples, showed no sign of radioisotopes and contained almost no sediment in both June and September (0.3-0.5 mg/L). With regards to microbiological parameters, CFU at 22°C exceeded the guideline limit in September, and coliform bacteria were detected, i.e. exceeded the guideline limit, in both June and September. Coliform bacteria showed high counts of 13 CFU mL^{-1} in September. The low inorganic content and relatively high microbiological content probably reflects the fact that all meltwater runs through a major lake probably with a long residence time.

L-10

Total catchment area of 22.2 km^2, including 14.9 km^2 of local ice cap area, with ice of late Holocene origin. Estimated mean discharge of 14,500 million litres per year, with the vast majority discharging from June to September. No apparent risk of outburst floods. L-10 had high sediment content in June (163 mg/L) and much lower in September (5 mg/L). In June, the sediment consisted mainly of fine silt, coarse silt and sand. A much lower water flow in September most likely explains at least some of this big change from June to September.

L-10 exceeded guideline limits for aluminum and nickel in unfiltered samples, but when sediment was removed, values were well below the limits. The stream showed no sign of radioisotopes. L-10 had high sediment content in June (163 mg/L) and much lower in September (5 mg/L). A much lower water flow in September most likely explains at least some of this big change from June to September. In June, the sediment consisted mainly of fine silt, coarse silt and sand. The poor sorting of the sediment probably reflects that part of the water runs through some minor lakes and other parts do not run through lakes. With regards to microbiological parameters, CFU at 22°C and coliform bacteria exceeded the guideline limit in September.

9. References

Ahlstrøm, A. P., Albers, C. N., Andersen, S. B., Andresen, C. S., Van As, D., Citterio, M., Fausto, R. S., Hansen, K., Hasholt, B., Johnsen, A. R., Kjeldsen, K. K. & Solgaard, A. M. 2018: Greenlandic Ice Cap Water – Technical Report on five potential locations for meltwater export. Geological Survey of Denmark and Greenland Report 2018/29, 51pp.

Aschwanden, A., Bueler, E., Khroulev, C. and Blatter, H. 2012: An enthalpy formulation for glaciers and ice sheets. Journal of Glaciology **58**(208), 441–457.

Bekendtgørelse om naturligt mineralvand. kildevand og emballeret drikkevand" (BEK nr 38 af 12/01/2016).

bkg_nr_07 2008_bilag3a_dk pdf (analyseprogram kemiske parametre for Grønlandsk drikkevand). Fra: Hjemmestyrets bekendtgørelse nr. 7 af 17. marts 2008 om vandkvalitet og tilsyn med vandforsyningsanlæg.

bkg_nr_07 2008_bilag1b_dk pdf (generelle og uorganiske parametre i Grønlandsk drikkevand). Fra: Hjemmestyrets bekendtgørelse nr. 7 af 17. marts 2008 om vandkvalitet og tilsyn med vandforsyningsanlæg.

Bueler, E. & Brown, J. 2009: Shallow shelf approximation as a "sliding law" in a thermodynamically-coupled ice sheet model. Journal of Geophysical Research Atmospheres **114**, F03008, doi:10.1029/2008JF001179.

Callieri, C., Cronberg, G. & Stockner, J. Chapter 8: Freshwater picocyanobacteria: Single cells. Microcolonies and colonial forms. In Ecology of Cyanobacteria II: Their Diversity in Space and Time; Whitton. B.A.. Ed.; Springer: Dordrecht. The Netherlands. 2012; pp. 229–261.

Chang, C. L., Jeong, J., Shin, J. H., Lee, E. Y. & Son, H. C. 1999: *Rahnella aquatilis* Sepsis in an Immunocompetent Adult. Journal of Clinical microbiology 37: 4161–4162.

Citterio, M. & Ahlstrøm, A. 2013: *Brief communication:* The aerophotogrammetric map of Greenland ice masses. The Cryosphere, **7**(2), 445–449, doi:10.5194/tc-7-445-2013.

Dee, D. P., Uppala, S. M., Simmons, A. J., Berrisford, P., Poli, P., Kobayashi, S., et al. 2011: The ERA-Interim reanalysis: configuration and performance of the data assimilation system. Q.J.R. Meteorol. Soc. 137, 553–597. doi:10.1002/qj.828.

Donnenberg, M.S. 2010: Enterobacteriaceae. In: Eds. Bennett JE, Dolin R. Principles and Practice of Infectious Diseases. 7th. Vol2:2815-2833, Elsevier, Philadelphia PA.

DS/EN ISO 6222:2000. Vandundersøgelse. Bestemmelse af antal mikroorganismer i gærekstraktagar ved 22°C og 36°C. Dybdeudsæd.

DS/EN ISO 9308-1:2014 Water quality – Enumeration of Escherichia coli and coliform bacteria.

EPA. 2016: Ground Water and Drinking Water. Table of Regulated Drinking Water. Contaminents. 15pp.

EU. 2013: Rådets Direktiv 2013/51/EURATOM af 22. Oktober 2013 om krav til beskyttelse af befolkningens sundhed med hensyn til radioaktive stoffer i drikkevand. 10pp.

Ettema, J., Van den Broeke, M. R., Van Meigaard, E., Van de Berg, W. J., Bamber, J. L., Box, J. E. & Bales, R. C. 2009: Higher surface mass balance of the Greenland ice sheet revealed by high-resolution climate modeling. Geophys. Res. Lett., **36**, L12501, doi:10.1029/2009GL038110.

Fettweis, X., Box, J. E., Agosta, C., Amory, C., Kittel, C., Lang, C., van As, D., Machguth, H. & Gallée, H. 2017: Reconstructions of the 1900–2015 Greenland ice sheet surface mass balance using the regional climate MAR model. The Cryosphere, **11**, 1015–1033, https://doi.org/10.5194/tc-11-1015-2017.

Harrell. L. J., Cameron, M. L., O'Hara, C. M. 1989: *Rahnella aquatilis*, an unusual gram-negative rod

isolated from the bronchial washing of a patient with acquired immunodeficiency syndrome. Journal of Clinical Microbiology **27**:1671–1672.

Hock , R. 1999: A distributed temperature-index ice- and snowmelt model including potential direct solar radiation. Journal of Glaciology, 45, 149.

Howat, I. M., Negrete, A. & Smith, B. E. 2014: The Greenland Ice Mapping Project (GIMP) land classification and surface elevation data sets. The Cryosphere, **8**, 1509–1518, https://doi.org/10.5194/tc-8-1509-2014.

International Council of Bottled Water Associations standards. ICBWA Model Code. September 27. 2004.

Janssens, I. & Huybrechts, P. 2000: The treatment of meltwater retention in mass-balance parameterizations of the Greenland ice sheet. Annals of Glaciology 31, 133–140.

Kjeldsen, K. K., Ahlstrøm, A. P., Albers, C. N., Larsen, S. H., Johnsen, A. R., Andersen, S. B., Andresen, C. S., Citterio, M., Fausto, R. S., Solgaard, A. M. 2019: Revised assessment of potential locations for export of meltwater from the glaciers in Greenland. Geological Survey of Denmark and Greenland Report 2019/37 (confidential to be released 01.01.2025), 37pp.

Korsgaard, N. J., Nuth, C., Khan, S. A., Kjeldsen, K. K., Bjørk, A. A., Schomacker, A. & Kjær, K. H. 2016: Digital elevation model and orthophotographs of Greenland based on aerial photographs from 1978-1987. Sci. Data, **3**, doi:10.1038/sdata.2016.32.

Kuzdan, C., Soysal, A., Özdemir, H., Coşkun, Ş., Akman, İ., Bilgen, H., Özek, E., Bakır, M. 2015: Rahnella aquatilis Sepsis in a Premature Newborn. Case Reports in Pediatrics. Volume 2015, Article ID 860671. http://dx.doi.org/10.1155/2015/860671.

Mayer, C. J., Bøggild, C. E., Olesen, O. B. & Podlech, S. 2003: Ice studies in relation to ice/water export, data collection, modelling and evaluation approach. Danmarks og Grønlands Geologiske Undersøgelse Rapport 2003/6, 33pp.

Pfeffer, W. T. et al. 2014: The Randolph Glacier Inventory: a globally complete inventory of glaciers, , **60**(221), 537–552, doi:10.3189/2014JoG13J176.

Reeh, N., Oerter, H. & Thomsen, H. H. 2002: Comparison between Greenland ice-margin and ice-core oxygen-18 records. Annals of Glaciology, **35**, 136-144, https://doi.org/10.3189/172756402781817365.

Rozhon, W., Petutschnig, E., Khan, M., Summers, D. K., Poppenberger, B. 2010: Frequency and diversity of small cryptic plasmids in the genus *Rahnella*. BMC Microbiology **10**, Article number: 56.

Steenfelt, A. 1999: Compilation of data sets for a geochemical atlas of West and South Greenland based on stream sediment surveys 1977 to 1997. Danmarks og Grønlands Geologiske Undersøgelse Rapport 1999/41, 33 pp.

Tash, K. 2005: *Rahnella aquatilis* Bacteremia from a Suspected Urinary Source. Journal of Clinical Microbiology **43**:2526-2528. doi: 10.1128/JCM.43.5.2526-2528.2005

Trout-Haney, J. V., Wood, Z. T. & Cottingham, K. L. 2016: Presence of the Cyanotoxin Microcystin in Arctic Lakes of Southwestern Greenland. Toxins **8**: 256, doi:10.3390/toxins8090256.

Vincent, W. R. & Quesada, A. Chapter 13: Cyanobacteria in high latitude lakes, Rivers, and seas. In Ecology of Cyanobacteria II: Their Diversity in Space and Time; Whitton. B.A.. Ed.; Springer: Dordrecht. The Netherlands. 2012; pp. 229–261.

WHO. 1999: Toxic Cyanobacteria in Water: A guide to their public health consequences. monitoring and management. Edited by Ingrid Chorus and Jamie Bartram. http://www.who.int/water_sanitation_health/resourcesquality/toxcyanobacteria.pdf.

WHO. 2011. Guidelines for Drinking-water Quality. Fourth edition.

Wikipedia downloaded 27/11-2019; https://en.wikipedia.org/wiki/Acinetobacter)

Winkelmann, R., Martin, M. A., Haseloff, M., Albrecht, T., Bueler, E., Khroulev, C. & Levermann, A. 2011:

The Potsdam Parallel Ice Sheet Model (PISM-PIK) Part 1: Model description. The Cryosphere, **5** 715-726.

10. Appendix A

Threshold values (max values) for inorganic parameters in relevant regulations and guidelines concerning drinking water. No value means that the parameter is not included in the regulation/guideline. All concentrations are in mg/L. Parameters in *italic* have not been analyzed on the localities.

	Tap water				**Bottled water**	
Parameter	Drikkevand (GL)[1)]	Drikkevand (DK)[2)]	Drikkevand (EU)[3)]	Drikkevand (USA)[4)]	Naturligt mineralvand (DK)[5)]	ICBWA[6)]
Aluminum	0.20	0.20	0.20	0.20		
Ammonium	*0.5*	*0.05*	*0.5*			
Antimony	0.005	0.005	0.005	0.006	0.005	0.005
Arsenic	0.005	0.010	0.010	0.010	0.010	0.010
Barium		0.700		2	1.0	
Beryllium		*0.010*		*0.004*		
Lead	0.010	0.010	0.010		0.010	0.010
Boron	1.0	1.0	1.0			0.3
Cadmium	0.005	0.005	0.005	0.005	0.003	0.003
Chromium	0.050	0.050	0.050	0.1	0.050	0.05
Cyanide	*0.050*	*0.050*	*0.050*	*0.2*	*0.070*	*0.07*
Fluoride	1.5	1.5	1.5	4	5.0	1.5
Iron	*0.2*	*0.2*	*0.2*	*0.3*		
Copper	2.0	2.0	2.0	1.3	1.0	2.0
Cobalt		0.005	0.005			
Magnesium		50				
Manganese	*0.05*	*0.05*	*0.05*	*0.05*	*0.50*	*0.05*
Mercury	0.001	0.001	0.001	0.002	0.001	0.001
Molybdenum		*0.020*				*0.070*
Sodium	200	175	200			
Nickel	0.020	0.020	0.020		0.020	0.020
Nitrate	50	50	50	44	50	221
Nitrite	*0.5*	*0.1*	*0.5*	*3.3*	*0.1*	*10*
Selenium	0.010	0.010	0.010	0.050	0.010	0.010
Sulfate	250	250	250	250		
Thallium		*0.001*		*0.002*		
Zink	0.100	0.100				
pH	6.5-9.5	7.0-8.5	6.5-9.5	6.5-8.5*		6.5-8.0
Conductivity	<250 mS/m	>30 mS/m*	<250 mS/m			

[1)] Hjemmestyrets bekendtgørelse nr. 7 af 17. marts 2008

[2)] Ved taphane hos forbrugeren (BEK nr 1310 af 25/11/2015)

[3)] RÅDETS DIREKTIV 98/83/EF

[4)] US safe drinking water act (National Primary Drinking Water Regulations)

[5)] BEK nr 38 af 12/01/2016

[6)] The International Council of Bottled Water Associations Standards

* Suggested value – not a criterion